Detrital zircon ages: A key to unraveling provenance variations in the eastern Yinggehai–Song Hong Basin, South China Sea

Article *in* AAPG Bulletin · July 2019

DOI: 10.1306/11211817270

6 authors, including:

Ce Wang
Sun Yat-Sen University
27 PUBLICATIONS 211 CITATIONS

Xirong Liang
Chinese Academy of Sciences
36 PUBLICATIONS 1,479 CITATIONS

Chuanxin Tong
China National Offshore Oil Corporation
14 PUBLICATIONS 152 CITATIONS

Detrital zircon ages: A key to unraveling provenance variations in the eastern Yinggehai–Song Hong Basin, South China Sea

Ce Wang, Xinquan Liang, David A. Foster, Xirong Liang, Chuanxin Tong, and Ping Liu

ABSTRACT

The Yinggehai–Song Hong Basin has received a large amount of terrigenous sediment from different continental blocks since the Paleogene. The Yingdong slope, which is located on the eastern side of this basin, is an important potential gas province, but the provenance of the marine sediments in this area are poorly understood. The detrital zircon U-Pb geochronology of sedimentary rocks from the lower Miocene to Quaternary is examined in this study to investigate the temporal and spatial variations in provenance since the early Miocene. The U-Pb ages of detrital zircon range from 3078 to 30 Ma, suggesting that sediment input is derived from multiple sources. Detailed analyses of these components indicate that both the Red River and Hainan are likely the major sources of the sediments on the Yingdong slope, with additional minor contributions from central Vietnam (eastern Indochina block) and possibly the Songpan–Garze block. Variations in the dominant detrital zircon populations within stratigraphic successions display an increasing contribution from the Red River since the middle Miocene. This resulted from the progradation of the Red River Delta in the northern basin and may have also been influenced by regional surface uplift and associated climate changes in East Asia. This study shows that the Red River has had a relatively stable provenance since at least the early Miocene, indicating that any large-scale drainage capture of the Red River should have occurred before circa 23 Ma.

Manuscript received June 28, 2017; provisional acceptance August 4, 2017; revised manuscript received October 16, 2017; revised manuscript provisional acceptance January 9, 2018; 2nd revised manuscript received March 20, 2018; 2nd revised manuscript provisional acceptance June 5, 2018; 3rd revised manuscript received June 11, 2018; 3rd revised manuscript provisional acceptance July 10, 2018; 4th revised manuscript received July 12, 2018; final acceptance November 21, 2018.
DOI:10.1306/11211817270

AUTHORS

Ce Wang ~ *State Key Laboratory of Isotope Geochemistry, Guangzhou Institute of Geochemistry, Chinese Academy of Sciences, Guangzhou, China; wangce@gig.ac.cn*

Ce Wang is a young geologist at the State Key Laboratory of Isotope Geochemistry, Guangzhou Institute of Geochemistry, Chinese Academy of Sciences. He received his B.Sc. in geology from the Guilin University of Technology and his Ph.D. in geology from the University of Chinese Academy of Sciences. His research interests include sedimentology, hydrocarbon reservoirs, and tectonic evolution.

Xinquan Liang ~ *State Key Laboratory of Isotope Geochemistry, Guangzhou Institute of Geochemistry, Chinese Academy of Sciences, Guangzhou, China; liangxq@gig.ac.cn*

Xinquan Liang is a professor at the Guangzhou Institute of Geochemistry, Chinese Academy of Sciences. He received his B.Sc. in geology from the Changchun College of Geology and his M.Sc. and Ph.D. from the Chinese Academy of Sciences. His current research interests are focused on basin analysis, metallogeny, and sedimentary geology. Xinquan Liang is the corresponding author of this paper.

David A. Foster ~ *Department of Geological Sciences, University of Florida, Gainesville, Florida; dafoster@ufl.edu*

David A. Foster is a professor of geology and chair of the Department of Geological Sciences at the University of Florida. He received his Ph.D. from the University of New York at Albany. His current research interests include tectonics, thermochronology, and geochronology.

Xirong Liang ~ *State Key Laboratory of Isotope Geochemistry, Guangzhou Institute of Geochemistry, Chinese Academy of Sciences, Guangzhou, China; xrliang@gig.ac.cn*

Xirong Liang is a professor at the State Key Laboratory of Isotope Geochemistry, Guangzhou Institute of Geochemistry, Chinese Academy of Sciences. He received his Ph.D.

from the Chinese Academy of Sciences. His research focuses on igneous petrology and geochemical and isotopic geology.

Chuanxin Tong ~ *Zhanjiang Branch, China National Offshore Oil Corporation, Ltd., Zhanjiang, China; tongchx@cnooc.com.cn*

Chuanxin Tong is a geologist in the Zhanjiang Branch of the China National Offshore Oil Corporation, Limited. He received his M.Sc. from the Chengdu University of Technology. He is a manager in the company and specializes in petroleum systems, especially hydrocarbon migration and accumulation in high-temperature and high-pressure basins.

Ping Liu ~ *Zhanjiang Branch, China National Offshore Oil Corporation, Ltd., Zhanjiang, China; liuping7@cnooc.com.cn*

Ping Liu is a geologist in the Zhanjiang Branch of the China National Offshore Oil Corporation, Limited. She received her Ph.D. in geochemistry from the Guangzhou Institute of Geochemistry, Chinese Academy of Sciences. She is now an engineer in the company and specializes in understanding sedimentary geochemistry and its application in reservoir modeling and simulation.

ACKNOWLEDGMENTS

We would like to acknowledge Peter Clift, Long Van Hoang, Upendra Baral, Chao Lei, two anonymous reviewers, and AAPG Editor Barry J. Katz for their helpful comments and constructive suggestions. We acknowledge the China National Offshore Oil Corporation, Zhanjiang Branch, for assisting with this research and supplying the samples. This research was funded by the National Natural Science Foundation of China (41702115 and 41576040), China Postdoctoral Science Foundation–Chinese Academy of Sciences Joint Foundation for Excellent Postdoctoral Fellows (2016LH00022), China Postdoctoral Science Foundation (2016M602551), and Natural Science Foundation of Guangdong Province of China (2017A030313250).

DATASHARE 108

Table S1 is available in an electronic version on the AAPG website (www.aapg.org/datashare) as Datashare 108.

INTRODUCTION

Provenance studies can offer crucial constraints on drainage scales and sediment pathways in ancient depositional systems (Cawood et al., 2004; Hallsworth and Chisholm, 2008) and aid in the prediction of sandstone distribution and reservoir quality in petroliferous basins (Fontanelli et al., 2009). Clastic sedimentary rocks may contain important information regarding their provenance and sedimentary processes during deposition (Benyon et al., 2016) and can thus be used to investigate the spatial and temporal variations in source evolution and depositional history (Cawood and Nemchin, 2000; Lowe et al., 2011). Different source terranes will yield detrital zircons with U-Pb ages indicative of the zircon ages within the crystalline and sedimentary rocks that may be unique enough to assess sediment provenance and associated changes (Cawood et al., 2003; DeCelles et al., 2004; Liang et al., 2008; Clift et al., 2012; Bracciali et al., 2015).

The Yingdong slope within the Yinggehai–Song Hong (Y-SH) Basin (Figure 1) is an important target of potential hydrocarbon exploration, but no consensus has been reached regarding the origin of the sedimentary rocks and contributions of different source terranes (Wang et al., 2014). Numerous factors can control the distribution of hydrocarbon reservoirs, such as the depositional environment, diagenesis, sediment distribution, and nature of the source region (Morton et al., 2008; Wang et al., 2016a). Analyzing the provenance of this region is crucial, therefore, to understand the paleogeography and improve predictions of reservoir properties (He et al., 2005).

Previous studies using seismic profiles and petrographic data sets from sandstones (e.g., Gong et al., 1997; Clift and Sun, 2006; Xie, 2009; Lei et al., 2015) proposed that the Truong Son belt in the Indochina block (central Vietnam), the hinterland of the southern Yangtze block (Yunnan Province of China), and the Hainan uplift in the Cathaysia block (Hainan Island) are all potential source terranes for the Y-SH Basin (Figure 1). However, these study methods had some inherent and critical shortcomings because they could not effectively identify, characterize, or determine the potential source terranes. The proximity of the Yingdong slope in the eastern Y-SH Basin to Hainan Island makes this island an obvious potential sediment source for this region (Figure 1). For instance, Gong et al. (1997) and Xie (2009) analyzed heavy minerals and seismic profiles to constrain the provenance and suggested that Hainan was the main source terrane for this region. Based on the presence of zircon with ages from the late Permian to Cretaceous, Yan et al. (2011) proposed that sedimentary rocks in the Yingdong slope were mainly derived from Hainan. Nevertheless, recently published heavy mineral, detrital zircon U-Pb dating, and Nd and Pb isotope provenance studies revealed that these sedimentary rocks were probably derived

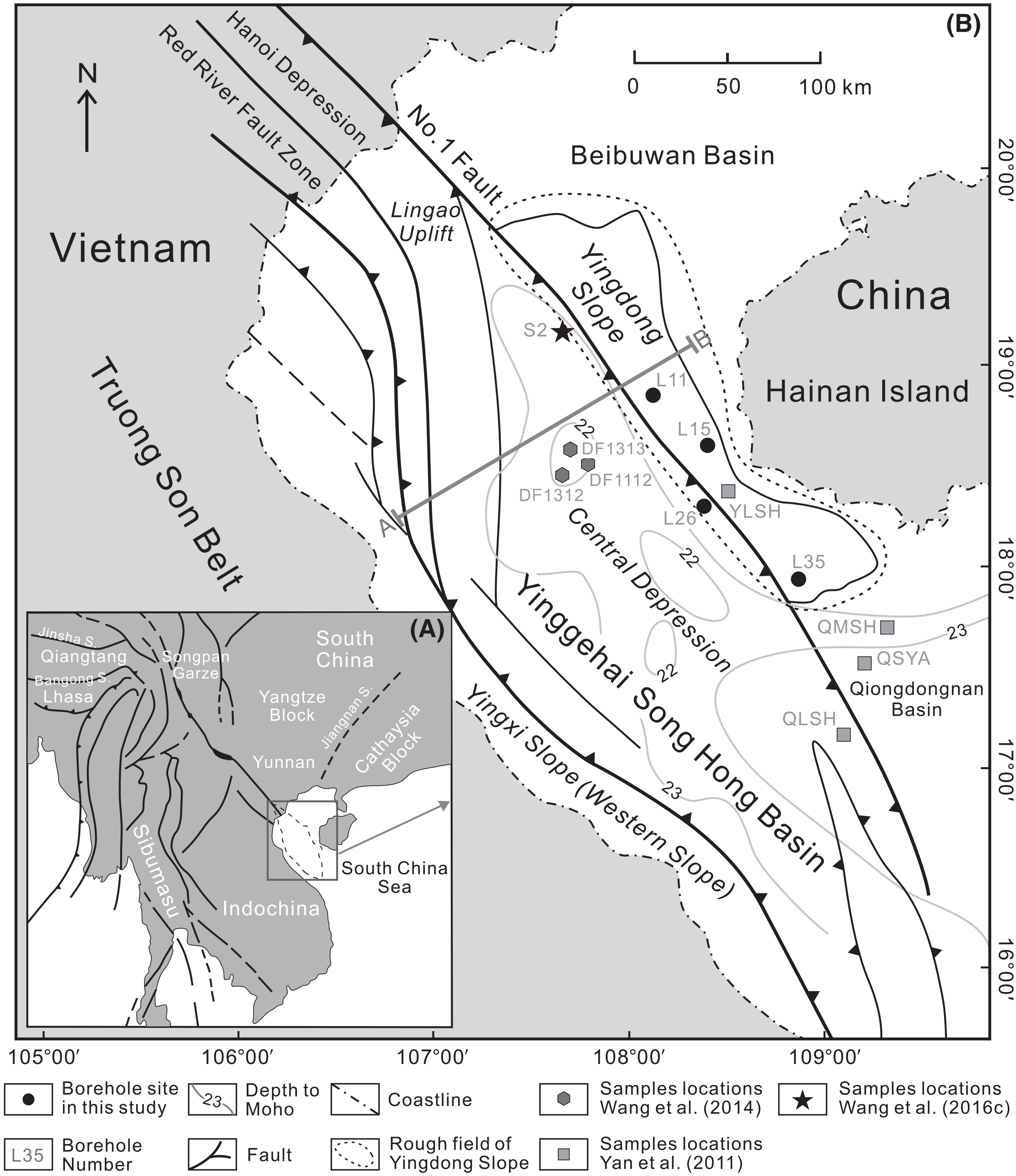

Figure 1. (A, B) Geologic map and borehole locations of the Yinggehai–Song Hong Basin. The Moho depth in the map is based on seismic analysis from the China National Offshore Oil Corporation and was adapted after He et al. (2002) and Zhu and Lei (2013). L11, L15, L26, and L35 are the borehole names. DF1112, DF1312, DF1313, QLSH, QMSH, QSYA, and S2 are the sample names.

from the Red River (southern Yangtze block) and central Vietnam (eastern Indochina block) rather than from Hainan to the east (Clift et al., 2006b, 2008; Jiang et al., 2015; Wang et al., 2016a). In recent years, studies of modern river sediments and outcropping bedrock in potential source areas around the Y-SH Basin showed that well-defined detrital zircon populations from the Red River are fundamentally different from those from central Vietnam and Hainan (Clift et al., 2006a; Hoang et al., 2009; Wang et al., 2014; Jonell et al., 2017). These studies suggest that geochronological information is well suited to assess the sedimentary provenance in this basin (Yan et al., 2011; Jiang et al., 2015).

Surface uplift changes continental topographic gradients and can influence regional drainage patterns, which may control the discharge of eroded sediments to the ocean (Clift et al., 2002, 2008; Liang et al., 2008). The Red River, which is the dominant river system that transports sediments from eastern Tibet and southern China to the South China Sea, has been proposed to have progressively lost its headwater drainage because of Cenozoic drainage reorganization that was caused by the uplift of the Tibetan Plateau (Brookfield, 1998; Clark et al., 2004; Clift et al., 2006b, 2008; Zheng et al., 2013). The timing of any major drainage reorganization is controversial and remains a major question. For example, mass balancing of eroded and sedimentary volumes indicated that the Red River catchment should have been much larger in the past than it is at present (Clift et al., 2006b). This model proposed that the upper reaches of the Yangtze (Jinshajiang), Salween, Irrawaddy, Mekong, and upper Brahmaputra (Yarlung) Rivers probably flowed into the head of the paleo–Red River and were diverted as the regional topography changed after the Tibetan uplift at the initiation of the Miocene (Clark et al., 2004). Other studies, such as Hoang et al. (2009), indicated that the Irrawaddy, Mekong, and Salween have never been connected to the paleo–Red River and inferred that any capture must have been pre-middle Miocene. Based on the Nd and Pb isotopic data, Clift et al. (2006b, 2008) indicated that drainage capture affected the Red River prior to circa 24 Ma. On the basis of ^{40}Ar-^{39}Ar ages from basalts along with detrital zircon U-Pb ages from sand, Zheng et al. (2013) suggested that the diversion of the upper and middle reaches of the Yangtze River away from the paleo–Red River must have occurred before 23 Ma. Drainage reorganization resulted from the regional extension of eastern China, strike-slip tectonism, and surface uplift in eastern Tibet. Based on detrital zircon U-Pb geochronological and paleogeographic data, Chen et al. (2017) suggested the existence of a paleo–Red River during the Paleocene to late Eocene, which lost its northern sources after circa 35 Ma. In addition, other observations negate the idea that large-scale river capture occurred in the geological past or predated the Oligocene (e.g., Yan et al., 2011; Zhao et al., 2015a; Wei et al., 2016; Wissink et al., 2016). Zhao et al. (2015a) found a more stable provenance from the Red River by geochemical data in the northwestern South China Sea and demonstrated no drainage capture for this drainage system since the late Oligocene. Wei et al. (2016) suggested that the upper Yangtze River had not been established until the late Miocene through the reconstruction of paleoflow, with no connection between the Red and Yangtze Rivers. Similarly, detrital zircon records in the Eocene to Pleistocene sedimentary basins indicated a stable fluvial system that was similar to the modern drainage network and excluded a link between the Yangtze and Red Rivers since at least the Eocene (Wissink et al., 2016). Large-scale drainage reorganization should affect the volume and composition of sedimentary rocks in basins (Clift et al., 2006b; Chen et al., 2017). If the drainage capture hypothesis is true, then the sediments that are transported to the Y-SH Basin may have changed over time, which should be displayed by distinct age populations of detrital zircons (Clift et al., 2006a; Hoang et al., 2009; Yan et al., 2011; Zheng et al., 2013).

In this study, we conducted detrital zircon U-Pb geochronology by means of laser ablation inductively coupled plasma mass spectrometry (LA-ICP-MS) to better understand the provenance of the Yingdong slope sedimentary rocks in the eastern Y-SH Basin, identify temporal and spatial variations in the sediment sources and contributions, and constrain the drainage evolution of the Red River since the Neogene.

GEOLOGICAL SETTING

The Y-SH Basin, which is located along the northern margin of the South China Sea continental shelf, is bounded by the Beibuwan Basin to the north and

Qiongdongnan Basin to the east (Figure 1). The Y-SH Basin is one of the most gas-rich sedimentary basins in the region, forming at the southeastern termination of the Red River strike-slip fault during the Cenozoic (Morley, 2002; Zhu and Lei, 2013), and it was the principal repository of eroded detritus from the Red River and its tributaries (Lei et al., 2015). The basin was filled with a thick section of Paleogene to Quaternary sedimentary rocks, which are up to 17 km (11 mi) thick in the Central depression (Gong et al., 1997; Yan et al., 2011), creating one of the thickest sedimentary sections on Earth. In addition to its large sediment volume, the basin is characterized by a high subsidence rate during the rifting stage, high overpressures, and widely developed diapirs in the central Yinggehai depression (Hao et al., 1995; Zhang et al., 1996; Huang et al., 2009; Lei et al., 2011). These characteristics have been recognized as important features for hydrocarbon exploration and production (Hao et al., 2000; Huang et al., 2004). The Y-SH Basin can be divided into four first-order tectonic units, namely, the Yingxi slope (Western slope), Central depression, Yingdong slope (Eastern slope), and Lingao uplift (Figure 1B). The primary strata boundaries can be effectively marked from the analysis and correlation of seismic sequences and nannofossil biostratigraphy (Duan and Huang, 1991). Numerous stratigraphic units that are related to hydrocarbon generation and accumulation can be further divided into the Lingtou Formation (Eocene); Yacheng and Lingshui Formations (middle and upper Oligocene, respectively); Sanya, Meishan, and Huangliu Formations (Miocene); and Yinggehai Formation (Pliocene). These units are covered by Quaternary sediments and underlain by a sub-Cenozoic basement (Figure 2).

The formation and development of the Y-SH Basin has been linked to the southeastward-oriented strike-slip deformation of the Ailao Shan–Red River fault zone (RRFZ) and clockwise rotation of the Indochina block (Guo et al., 2001; Sun et al., 2003; Zhu et al., 2009). The RRFZ extends over 1000 km (621 mi) between eastern Tibet and the South China Sea and is exposed as 10–20-km (6–12-mi)-wide belts of high-grade metamorphic and deformed granitic rocks (Gilley et al., 2003). Strike-slip motion along the fault zone has been widely regarded as compensation for the convergence between India and Asia (Tapponnier et al., 2001; Sun et al., 2003). Although controversial, the left-lateral strike-slip movement along the fault zone is dated to have occurred from 35 to 17 Ma based on stratigraphic and structural correlations, resulting in an offset between 500 and 1000 km (310–620 mi) (Leloup et al., 1995; Searle, 2006). However, the timing of reversal of slip within the RRFZ from 17 to 5 Ma is not well documented (Zhu et al., 2009). Pliocene–Quaternary right-lateral motion in the RRFZ occurred at 8–5 Ma, with the estimated slip ranging from several meters to 60 km (40 mi) (Leloup et al., 1995; Replumaz et al., 2001; Zhu and Lei, 2013). The evolution of the southeastern segment of the RRFZ in the offshore Tonkin Gulf area was divided into three stages by Rangin et al. (1995): (1) widespread left-lateral motion along the northwest-trending faults prior to circa 30 Ma; (2) localized left-lateral strike-slip within a 30-km-wide (20-mi-wide) area from 30 to 5.5 Ma, with the corresponding amount of offset not exceeding a few tens of kilometers; and (3) no detected tectonic activity after 5.5 Ma.

The Cenozoic tectonic evolution of the Y-SH Basin is divided into three periods: the synrift stage (Eocene to Oligocene), the postrift stage (middle–late Miocene), and a stage of renewed thermal subsidence (Pliocene to Holocene) (Figures 2 and 3) (Rangin et al., 1995; Gong et al., 1997; Lei et al., 2011). The basin began to open during the Eocene (after ca. 50 Ma) and then rapidly subsided after circa 34 Ma (Clift and Sun, 2006; Hoang et al., 2010b). The opening of the Y-SH Basin has often been linked to the large-scale left-lateral movement and clockwise rotation of the Indochina block along the RRFZ (Rangin et al., 1995; Guo et al., 2001), when the basin underwent a rifting period with northeast–southwest extension. The basin entered a postrifting period with limited tectonic activities since the Oligocene, although significant inversion occurred in the northern basin during the middle Miocene (Clift and Sun, 2006; Jiang et al., 2015). Three successive deformation phases were identified by high-resolution seismic reflection and borehole data, including left-lateral movement from 30 to 15.5 Ma, slip reversal between 15.5 and 5.5 Ma, and slow right-lateral movement after 5.5 Ma (Figure 2) (Zhu et al., 2009).

The intensification of the East Asian monsoon may be one of the most important factors that control continental weathering processes and, thus,

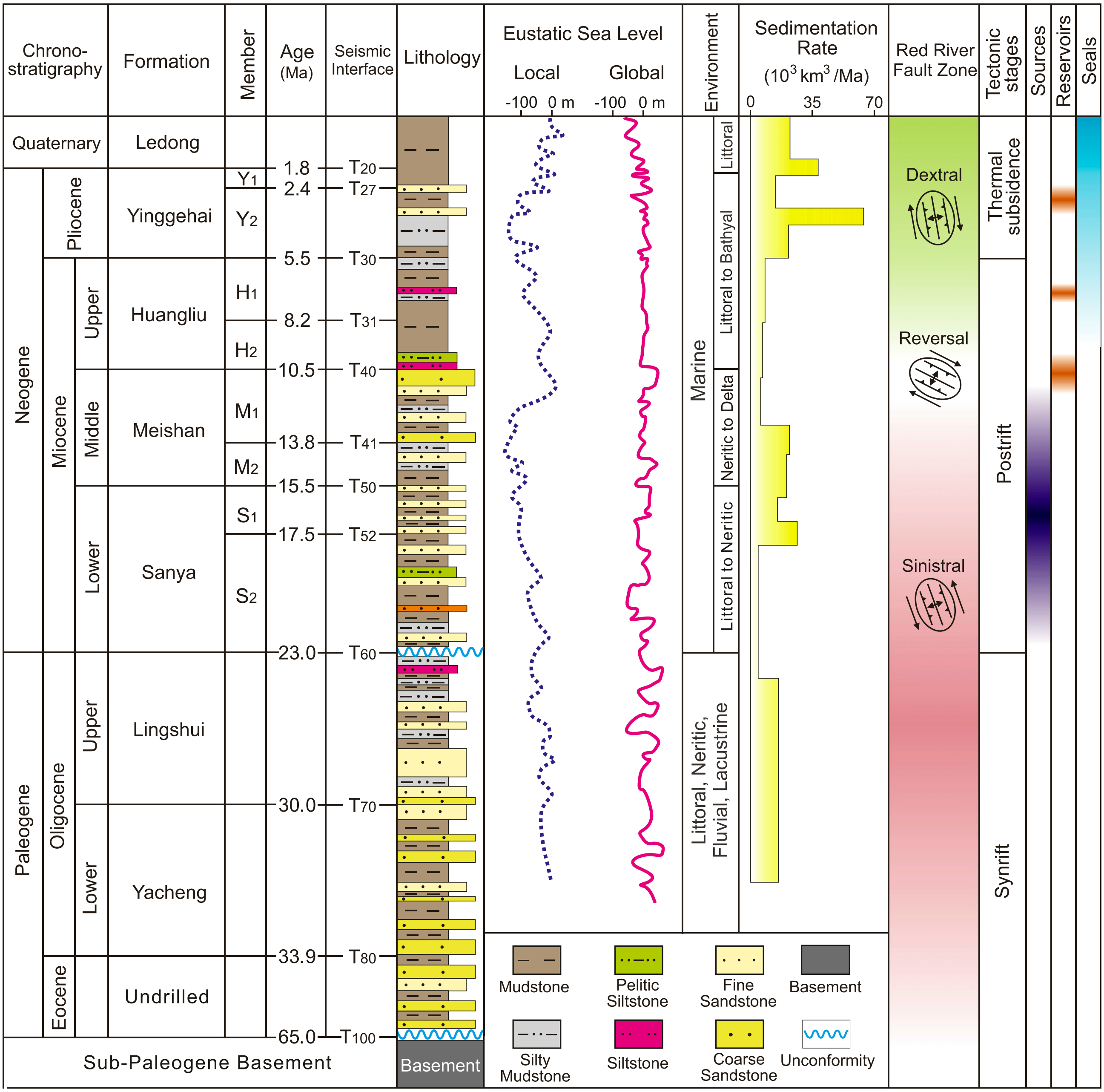

Figure 2. Regional stratigraphic column of the Yinggehai–Song Hong Basin, modified after Gong et al. (1997) and Liu et al. (2016). The global eustatic sea level is from Miller et al. (2005). The sedimentation rate for the basin is from Lei et al. (2015).

sedimentation (Wan et al., 2006). The inception age of the East Asia monsoon remains controversial, but has likely been established at least since the beginning of the Neogene (Clift et al., 2008), and significant variations in the monsoon system have occurred since, including the enhancement of aridity and monsoon intensity at circa 15–13, 8, and 3 Ma (Sun and Wang, 2005). On the basis of sedimentary records of the Y-SH and Qiongdongnan Basins, Hoang et al. (2010b) proposed that the initial intensification of the southeastern Asia monsoon occurred circa 22 Ma and was predominantly controlled by tectonic forces. Chemical weathering decreased since the Miocene, changing to more physical erosion and thus increasing sedimentation rates between 15.5 and 10 Ma. The monsoon intensity decreased from 10.5 to 3.3 Ma and increased again thereafter, consistent

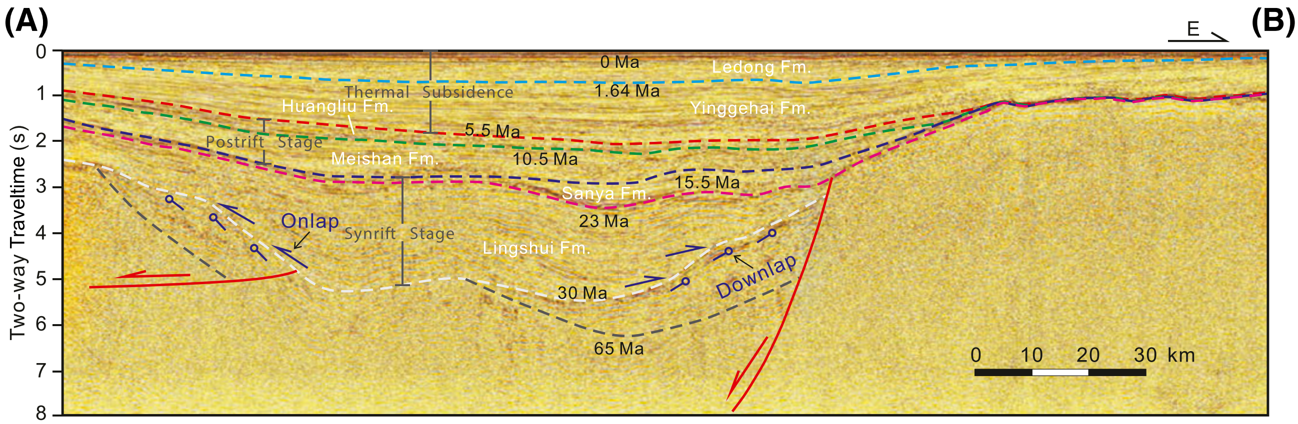

Figure 3. Interpreted seismic profiles across the Yinggehai–Song Hong Basin. The positions are shown in Figure 1 and modified after Zhu and Lei (2013). Fm. = Formation.

with the sediment flux to the ocean basins (Clift et al., 2008).

The depositional environments of the clastic sediments in the Paleogene to Quaternary deposits of the Y-SH Basin (Figure 2) vary over time, including lacustrine, fluvial, littoral, and neritic during the Eocene–Oligocene (before 23 Ma); littoral, delta, and neritic at the early–middle Miocene (30–10 Ma); and littoral and bathyal during the late Miocene to Quaternary (after 10 Ma) (Gong et al., 1997; Sun et al., 2003; Liu et al., 2016). The sedimentation rates were modest from 50 to 29.5 Ma, lower between 21 and 15.5 Ma, and higher from 15.5 to 10.5 Ma (Figure 2) (Clift and Sun, 2006; Hoang et al., 2010b), which is consistent with the Red River depositional system. Rapid erosion occurred in East Asia during the early–middle Miocene (24–11 Ma) (Clift and Sun, 2006) and was mostly related to the strengthening monsoon and tectonic rock uplift (Clift, 2006). Subsequently, the erosion rate gradually slowed but began to increase again during the late Pliocene and Pleistocene. The depocenters in the basin were mainly controlled by northwest- and roughly north-south–trending faults (Sun et al., 2003) and generally migrated to the southeast over time until being interrupted by fault reversal at circa 15.5 Ma. Inversion at 15.5 Ma produced an angular unconformity and caused the depocenters to migrate back to the northwest, pausing in the northwestern basin (Xie, 2009). The slowdown of right-lateral movement and high rates of sediment led to overspill into the neighboring Qiongdongnan Basin (Yan et al., 2011), and the depocenters again migrated southward (Zhu et al., 2009).

SAMPLING AND ANALYTICAL METHODS

Sampling

Ten sedimentary rocks were collected from four boreholes (L11, L15, L26, and L35) that were drilled by the China National Offshore Oil Corporation along the Yingdong slope in the eastern Y-SH Basin (Figure 1). Samples of fine- to coarse-grained sandstone and siltstone of 2–4 kg (4.4–8.8 lb) were collected in this study. The stratigraphic units of these samples range from the lower Miocene Sanya Formation to the Quaternary Ledong Formation (Figures 2 and 3). The detailed positions of the boreholes and information of the samples are shown in Figure 1 and Table 1, respectively.

Zircon U-Pb Isotopic Analysis by Laser Ablation Inductively Coupled Plasma Mass Spectrometry

The zircons were separated from 1 kg (2 lb) or greater samples by using conventional heavy liquid and magnetic separation techniques that were designed to minimize intersample cross-contamination (Rudnick and Williams, 1987). After hand sorting under a binocular stereoscope, the zircon grains were mounted in transparent epoxy and polished down to approximately half sections to expose the internal structures. Cathodoluminescence (CL) images were taken by using a Mono CL3 detector that was attached to an electron microprobe (JXA-8100, JEOL, Japan) to identify internal structures and choose potential target sites. Zircon grains were carefully observed

Table 1. Location and Stratigraphic Information of Samples Analyzed during This Study

Sample Number	Chronostratigraphy	Formation Units	Lithology	Borehole	Depth, m (ft)
L11-1	Quaternary	Ledong	Sandstone	L11	645 (2116)
L11-2	Pliocene	Upper Yinggehai	Siltstone	L11	750 (2461)
L11-4	Pliocene	Lower Yinggehai	Sandstone	L11	1680 (5512)
L11-5	Upper Miocene	Upper Huangliu	Sandstone	L11	1998 (6555)
L11-12	Upper Miocene	Lower Huangliu	Siltstone	L11	2150 (7054)
L15-1	Lower Miocene	Upper Sanya	Sandstone	L15	1104 (3622)
L15-3	Pliocene	Lower Yinggehai	Sandstone	L15	750 (2461)
L35-3	Pliocene	Upper Yinggehai	Sandstone	L35	720 (2362)
L35-4	Quaternary	Ledong	Siltstone	L35	520 (1706)
L26-5	Pliocene	Lower Yinggehai	Sandstone	L26	2020 (6627)

All the samples were collected from the core chips. The positions of borehole are shown in Figure 1.

to avoid any visible imperfections, such as inclusions and metamict zones, to avoid performing an analysis across zircon domain boundaries.

The zircons were dated by using LA-ICP-MS at the State Key Laboratory of Isotopic Geochemistry, Guangzhou Institute of Geochemistry, Chinese Academy of Sciences. Sample mounts were placed at the two-volume sample cell that had been flushed with Ar and He. Laser ablation was performed at a constant energy of 80 mJ (75,825 Btu) and a frequency at 8 Hz, with a spot diameter of 33 μm. The ablated ions were carried by He gas to the Agilent 7500a inductively coupled plasma mass spectrometry. Element corrections were made for mass bias drift, which was evaluated by reference to the glass standard NIST SRM 610. TEMORA was used as the age standard (^{206}Pb/^{238}U = 416.8 Ma). The details of the analytical operation and data processing procedures in this study were similar to those in Jackson et al. (2004). Isotopic ratios of U-Th-Pb were calculated with ICPMSDataCal (Version 7.2) (Liu et al., 2010). ^{206}Pb/^{238}U ages less than 1000 Ma were used, whereas ^{207}Pb/^{206}Pb ages were selected if the ^{206}Pb/^{238}U ages were older than 1000 Ma. Common Pb was corrected with ComPbCorr#3_151 by using the method of Andersen (2002). Probability diagrams for the zircon populations were constructed by using Kernel Density Estimation by Vermeesch (2012).

RESULTS

A total of 845 detrital zircon grains that were extracted from different stratigraphic units in the Yingdong slope were analyzed by LA-ICP-MS, including the cores and rims of the grains. The zircon grains were colorless to light pink and transparent, and their morphologies include a wide range of prismatic to oval-shaped crystals (Figure 4). The size of the zircon grains was generally 70–160 μm, and a proportion of these grains had subrounded or rounded corners. The euhedral grains generally suggest a relatively short transportation distance, whereas the rounded grains implied prolonged or multicycle transport. The U-Pb data are presented in detail in Table S1 (supplementary material available as AAPG Datashare 108 at www.aapg.org/datashare). Some grains displayed a typical metamorphic origin with low Th/U ratios (<0.1) (Table S1, supplementary material available as AAPG Datashare 108 at www.aapg.org/datashare), whereas most zircon grains had oscillatory growth zoning under CL (Figure 4) with overwhelmingly high Th/U values (>0.4) (Table S1, supplementary material available as AAPG Datashare 108 at www.aapg.org/datashare), suggesting a predominantly magmatic origin. The sedimentary rocks from the Yingdong slope can be roughly divided into two primary groups based on the detrital zircon U-Pb age populations (Figures 5 and 6): (1) those with complex populations of zircons, with U-Pb ages of circa 234–251, 420–445, 730–760, 940–970, 1600–1950, and 2420–2530 Ma and (2) those with significant bimodal age populations of circa 98 and 235–250 Ma.

Group 1: Samples L11-1, L11-2, L11-4, L11-12, L35-4, and L35-3

Sample L11-1 was collected from the Ledong Formation I in borehole L11. We analyzed 90 U-Pb

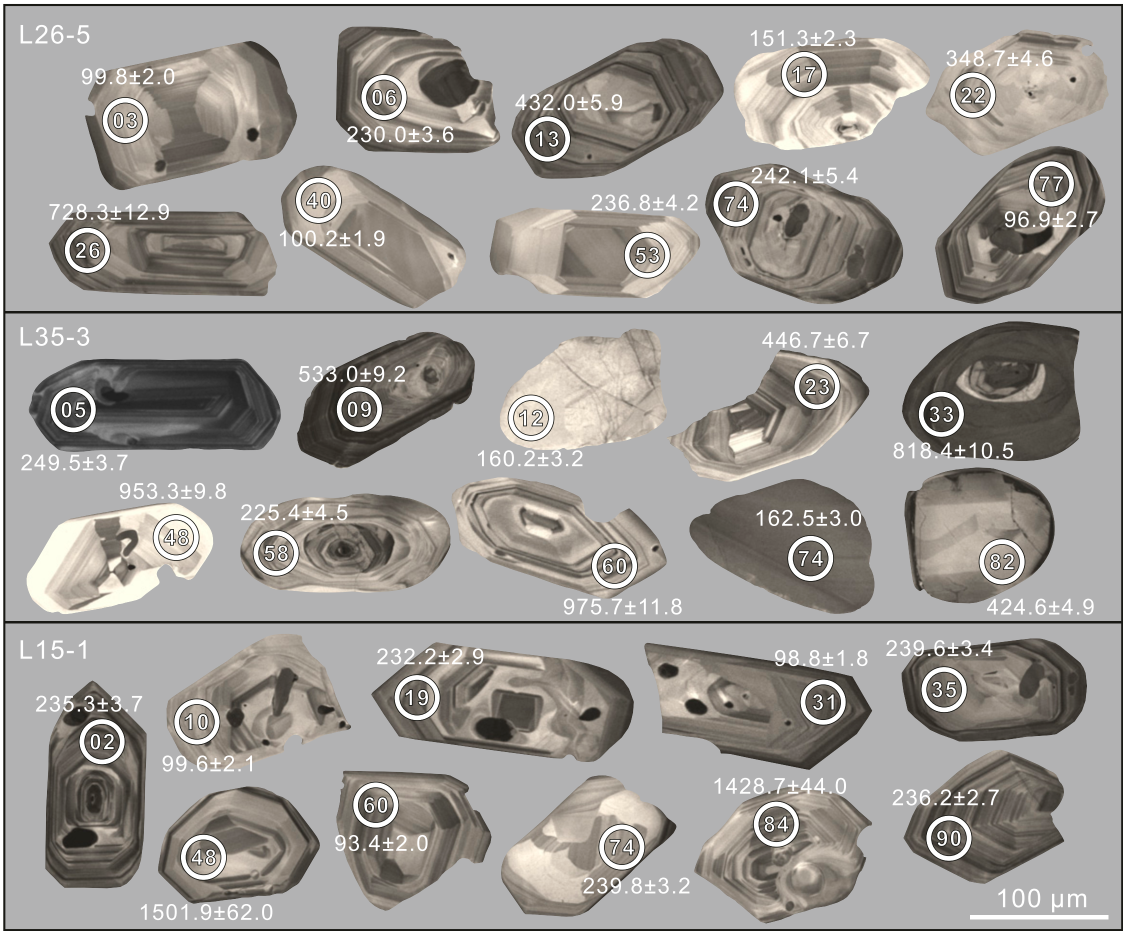

Figure 4. Cathodoluminescence images of representative detrital zircons from the U-Pb age analysis. The circles and numbers denote the laser ablation inductively coupled plasma mass spectrometry analytical spots and numbers, respectively. The numbers outside the circles are the zircon U-Pb ages.

spots on 90 zircon grains, 88 of which were concordant within uncertainties (>90%, the same below). The measured U-Pb ages ranged from 3078 to 30 Ma (Table S1, supplementary material available as AAPG Datashare 108 at www.aapg.org/datashare). The majority of the grains ranged between 200 and 450 Ma, with two primary peaks at circa 251 and 432 Ma, and several subordinate age peaks at circa 165, 749, 940, 1670, and 2420 Ma (Figure 5A).

Sample L11-2 was collected from the upper Yinggehai Formation in borehole L11. We analyzed 90 U-Pb spots on 90 zircon grains, 86 of which were concordant. The measured U-Pb ages ranged from 2984 to 82 Ma (Table S1, supplementary material available as AAPG Datashare 108 at www.aapg.org/datashare). Three major age peaks were observed at circa 100 Ma, 248 Ma, and 444 Ma, with a subordinate age peak at circa 159 Ma and one "broad" age group at 730–980 Ma (Figure 5B).

Sample L11-4 was collected from the lower Yinggehai Formation in borehole L11. All 80 analyses that were conducted on the 80 zircons from this sample were concordant within uncertainties. The measured U-Pb ages ranged from 2487 to 78 Ma (Table S1, supplementary material available as AAPG Datashare 108 at www.aapg.org/datashare), with one major age peak at circa 238 Ma and three subordinate peaks at circa 103, 439, and 1837 Ma (Figure 5C).

Sample L11-12 was collected from the lower Huangliu Formation in borehole L11. Of the 90 analyses that were conducted on the 90 zircons from this sample, 83 were concordant within uncertainties. The measured U-Pb ages ranged from 2606 to 99 Ma (Table S1, supplementary material available as AAPG Datashare 108 at www.aapg.org/datashare). Two

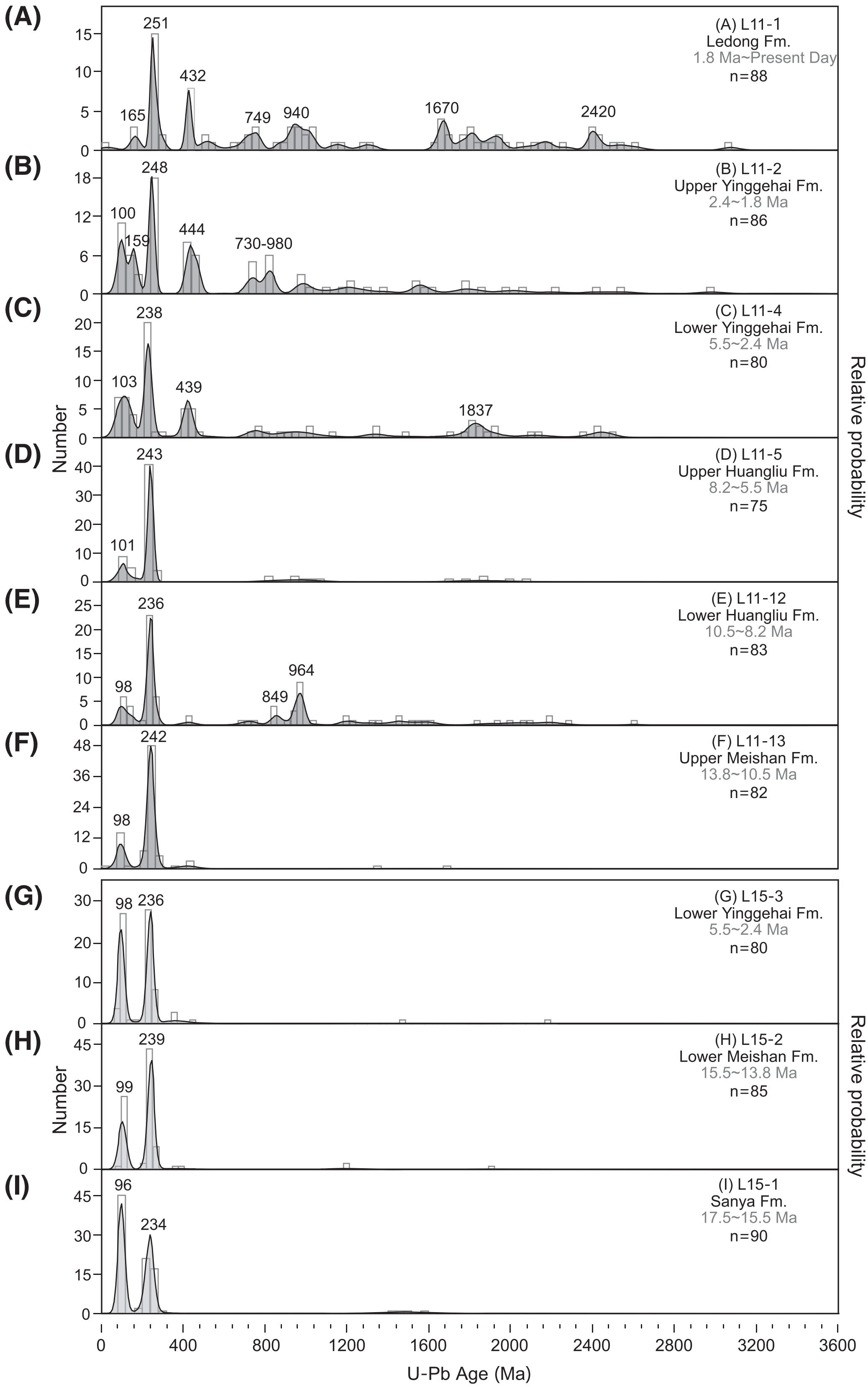

Figure 5. (A–I) Kernel density estimation plots of detrital zircons from boreholes L11 and L15. The data of L11-13 and L15-2 are from Wang et al. (2016a). Fm. = Formation.

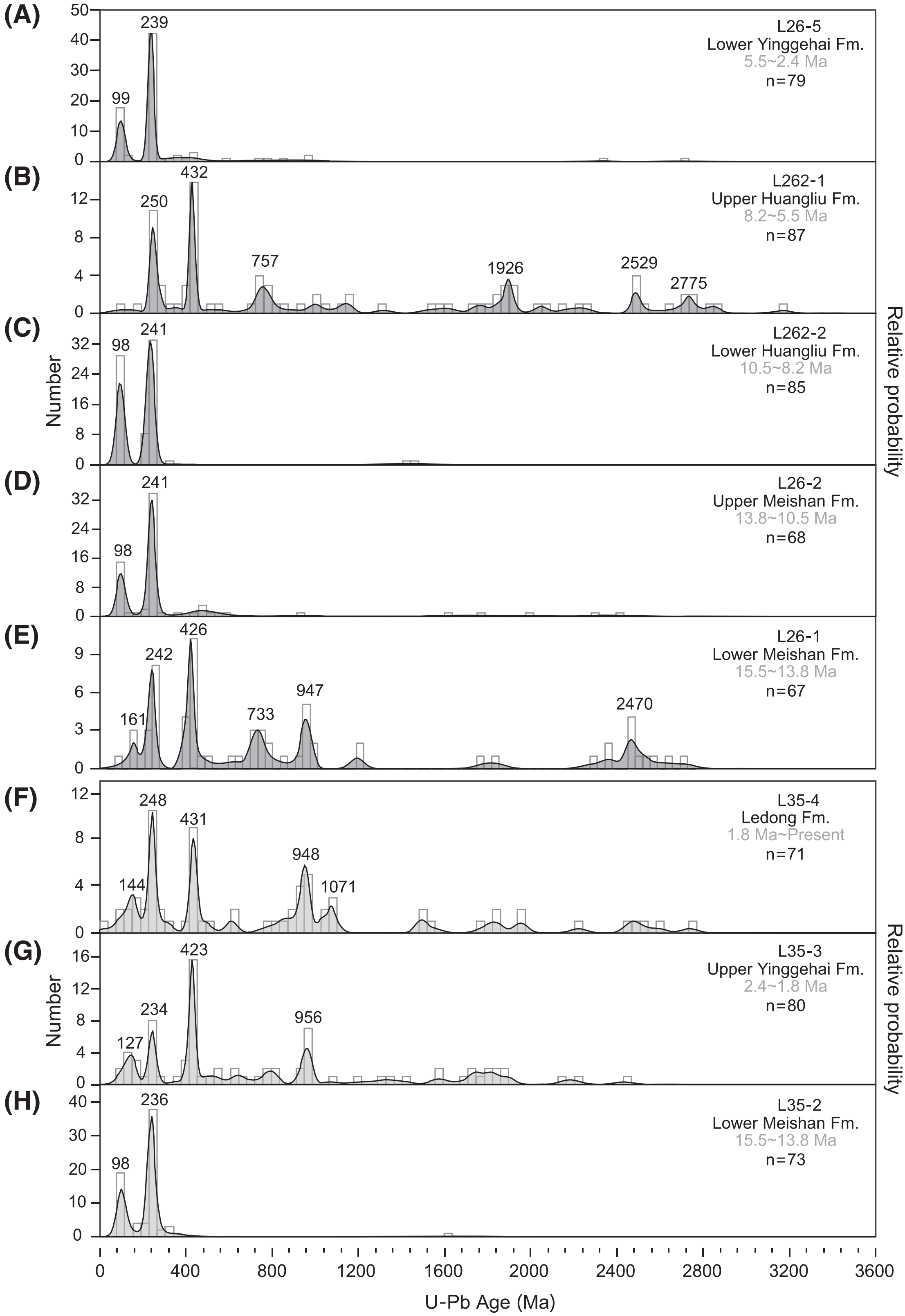

Figure 6. (A–H) Kernel density estimation plots of detrital zircons from boreholes L26 and L35. The data of L262-1 and L262-2 are from Wang et al. (2015a), and the data of L35-2, L26-2, and L26-1 are from Wang et al. (2016a). Fm. = Formation.

major age peaks were observed at circa 236 and 964 Ma, with two subordinate peaks at circa 98 and 849 Ma (Figure 5E).

Sample L35-4 was collected from the Ledong Formation in borehole L35. We analyzed 80 U-Pb spots on 80 zircon grains, and 71 of the analyses were concordant within uncertainties. The measured U-Pb ages ranged from 2739 to 32 Ma (Table S1, supplementary material available as AAPG Datashare 108 at www.aapg.org/datashare). Three major age peaks were observed at circa 248, 431, and 948 Ma, with two subordinate peaks at circa 144 and 1071 Ma (Figure 6F).

Sample L35-3 was collected from the upper Yinggehai Formation in borehole L35. Of the 85 analyses that were conducted on the 85 zircons from this sample, 80 were concordant within uncertainties. The measured U-Pb ages ranged from 2435 to 92 Ma (Table S1, supplementary material available as AAPG Datashare 108 at www.aapg.org/datashare). One major age peak was observed at circa 423 Ma, with three subordinate peaks at circa 127 Ma, 234 Ma, and 956 Ma (Figure 6G).

Group 2: Samples L11-5, L15-1, L15-3, and L26-5

Sample L11-5 was collected from the upper Huangliu Formation in borehole L11. We analyzed 80 U-Pb spots on 80 zircon grains, 75 of which were concordant. The measured U-Pb ages ranged from 2076 to 99 Ma (Table S1, supplementary material available as AAPG Datashare 108 at www.aapg.org/datashare). The majority of the grains ranged between 220 and 280 Ma, with one age peak at circa 243 Ma and a subordinate peak at circa 101 Ma (Figure 5D).

Sample L15-3 was collected from the lower Yinggehai Formation in borehole L15. We analyzed 80 U-Pb spots on 80 zircon grains, all of which were concordant. The measured U-Pb ages ranged from 2173 to 83 Ma (Table S1, supplementary material available as AAPG Datashare 108 at www.aapg.org/datashare). Two major age peaks were observed at circa 98 Ma and 236 Ma (Figure 5G).

Sample L15-1 was collected from the Sanya Formation in borehole L15. We analyzed 90 U-Pb spots on 90 zircon grains, all of which were concordant. The measured U-Pb ages ranged from 1567 to 86 Ma (Table S1, supplementary material available as AAPG Datashare 108 at www.aapg.org/datashare). This sample was similar to L15-3 and contained detrital zircons with two major age peaks at circa 96 and 234 Ma (Figure 5I).

Sample L26-5 was collected from the lower Yinggehai Formation in borehole L26. Of the 80 analyses that were conducted on the 80 zircons from this sample, 79 were concordant within uncertainties. The measured U-Pb ages ranged from 2706 to 96 Ma (Table S1, supplementary material available as AAPG Datashare 108 at www.aapg.org/datashare). Two major age peaks were observed at circa 99 and 239 Ma (Figure 6A).

DISCUSSION

Age Signatures of Possible Sediment Sources

The Truong Son belt in the Indochina block, the hinterland of the southern Yangtze block, and the Hainan uplift in the Cathaysia block (Figure 1) all constitute potential sedimentary sources for the Y-SH Basin (Gong et al., 1997; Yan et al., 2007, 2011; Cao et al., 2015; Jiang et al., 2015; Wang et al., 2015a). Increasing amounts of zircon geochronological data from modern sands in the major drainages and bedrock in these potential source terranes have been collected over the past decade and provide the basis to assess the provenance and tectonic evolution (e.g., Clift et al., 2006a; Hoang et al., 2009; Wang et al., 2015b; Jonell et al., 2017). The zircon U-Pb age spectra for the potential source terranes from the available published age data of major drainages and bedrocks are outlined in Figure 7. Generally, the zircon U-Pb ages from central Vietnam and Hainan show well-defined bimodal age spectra, whereas sources along the Red River (southern Yangtze block) exhibit relatively complex age populations.

The Yangtze block in the South China block is bounded to the north by the Qinling–Dabie orogenic belt and is adjacent to the Tibetan Plateau and Indochina block to the west and south, respectively (Figure 1A). The basement of the Yangtze block includes Proterozoic and Archean rocks with U-Pb zircon ages of circa 1700–2100 and 2300–2800 Ma,

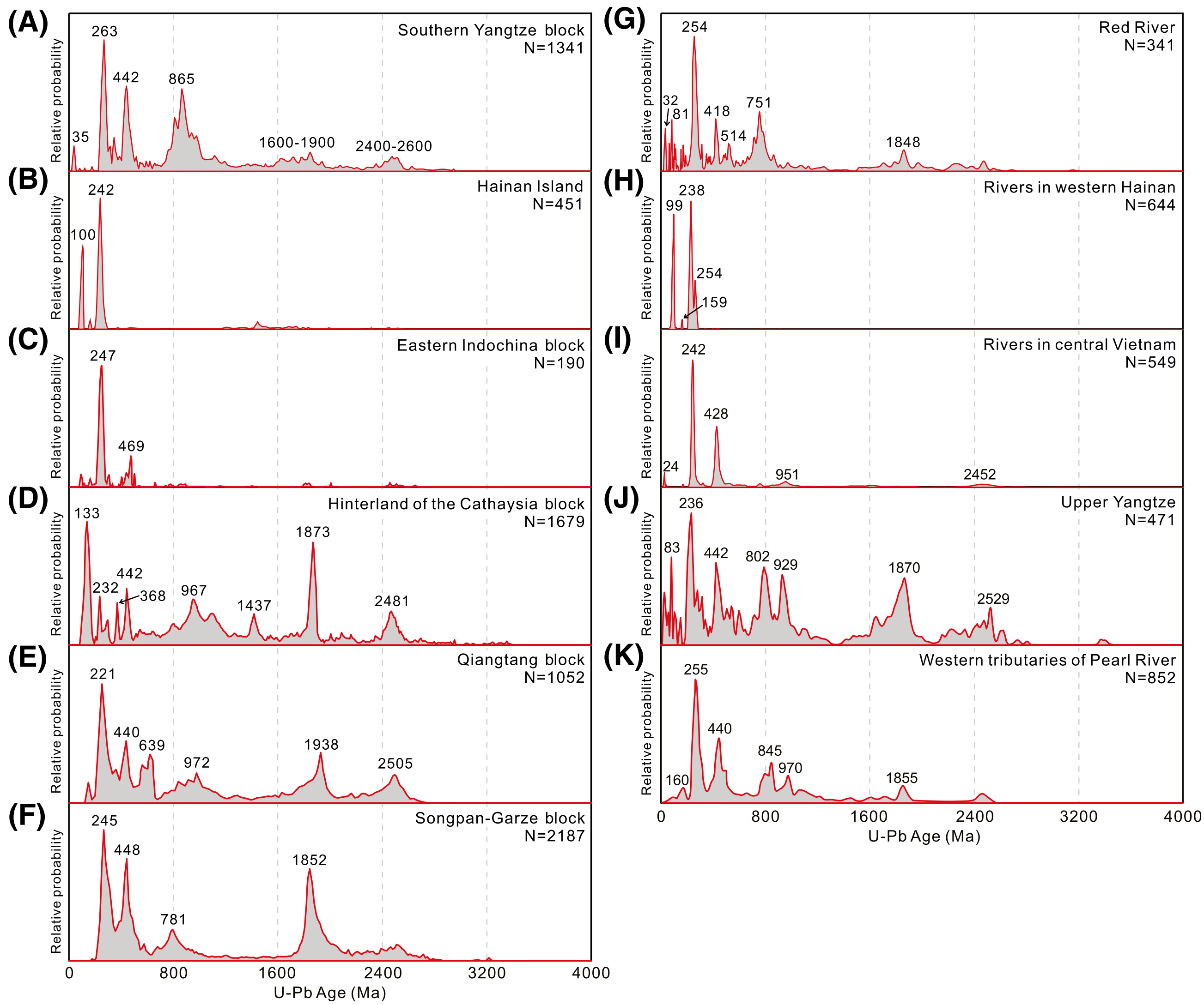

Figure 7. Zircon U-Pb age probability density plots of the bedrocks (A–F) and major drainages (G–K) of the potential source terranes. The data for the southern Yangtze block are from Zhang and Schärer (1999), Zhou et al. (2007), and Wang et al. (2007b). The data for Hainan Island are from Xie et al. (2006), Li et al. (2008), Xu et al. (2007a), and Wen (2013). The data for the eastern Indochina Block are from Carter et al. (2001), Roger et al. (2007), Liu et al. (2012), and Kamvong et al. (2014). The data for the hinterland of the Cathaysia block are from Wang et al. (2007a), Xu et al. (2007b), Yu et al. (2008), Yao et al. (2011), and Li et al. (2012). The data for the Qiangtang block are from Roger et al. (2003), Dong et al. (2011), and Ding et al. (2013). The data for the Songpan–Garze block are from Weislogel et al. (2006), Enkelmann et al. (2007), and Ding et al. (2013). The data for the Red River are from Clift et al. (2006a) and Hoang et al. (2009). Data for the rivers in western Hainan are from Wang et al. (2015b). The data for the rivers in central Vietnam are from Usuki et al. (2013) and Wang et al. (2016a). The data for the upper Yangtze are from Hoang et al. (2009), Kong et al. (2012), Yang et al. (2012), and He et al. (2013). The data for the western tributaries of the Pearl River are from Zhao et al. (2015b).

respectively (Zheng et al., 2006; He et al., 2013). The Neoproterozoic volcanic rocks, granitic plutons, and ophiolite complexes distributed around the Yangtze block are probably related to a mantle plume that marked the breakup of Rodinia and subsequent separation of the South China block between 1000 and 700 Ma (Li et al., 2003). Late Paleozoic igneous rocks are widespread in China's Yunnan Province and adjacent areas (Figure 1A) and yield U-Pb ages between 480 and 400 Ma (Carter et al., 2001; Liu et al., 2009; Wang et al., 2011). Permian to Triassic igneous rocks that are associated with the Emeishan mantle plume or collision between several microcontinents and the Yangtze block yielded ages from 280 to 220 Ma (Chen et al., 2014). Middle Jurassic to Cretaceous basaltic lavas and related mafic dikes, whose ages ranged from 180 to 80 Ma, are present in the southern Yangtze block (Li et al., 2004). The numerous magmatic and metamorphic rocks that are located in the southern Yangtze block along the RRFZ yielded U-Pb ages between 60 and 20 Ma (Zhang and Schärer, 1999) (Figure 7A).

Late Paleozoic to Mesozoic igneous rocks dominate Hainan Island, at the southern end of the Cathaysia block (Figure 1). Paleoproterozoic zircon with ages of circa 2600–2300 and 2000–1600 Ma are contained in the lower Paleozoic (Zhou et al., 2015). Mesoproterozoic volcaniclastic rocks related to the "Jinning movement" in the southern China block have been reported in western Hainan and exhibited ages of circa 1450 Ma (Li et al., 2008). The Permian to Triassic intrusive rocks in this region are predominantly high-K A-type and I-type granites and range in age from 280 to 220 Ma (Xie et al., 2006; Wen, 2013). Cretaceous granitic and volcanic rocks yielded zircon U-Pb ages of circa 100 and 160 Ma and are concentrated in southern Hainan (Zhou et al., 2015) (Figure 7B).

The Truong Son belt in the Indochina block (Figure 1) is characterized by Ordovician–Silurian and Permian–Triassic granitic and metamorphic rocks, which correspond to the Caledonian and Indosinian orogenic events, respectively. The lower Paleozoic granitoids within the Truong Son belt mainly occur in the southwestern region of the orogenic belt and yield ages of 430–460 Ma (Figure 7C) (Carter et al., 2001). Early Permian–Triassic arc magmatism (270–280 and 240–250 Ma) can be widely observed in the belt (Liu et al., 2012; Usuki et al., 2013). Furthermore, Archean to Neoproterozoic zircon grains have been discovered in the modern rivers and Paleozoic sedimentary rocks in central Vietnam (Usuki et al., 2013; Wang et al., 2016b; Jonell et al. 2017) (Figure 7I).

In addition to the above three primary potential source terranes, other possible sources that could have been delivered by the Red River system include the Qiangtang, Songpan–Garze, and hinterland of the Cathaysia blocks (Figure 1) (Van Hoang et al., 2009). These blocks are currently no longer part of drainage systems that are connected to the Y-SH Basin, so the detritus could not have been directly eroded but instead were recycled through sedimentary basins (Clift et al., 2006a). All three source terranes have relatively complex age populations, manifesting as multiple peaks (Figure 7D–F). The hinterland of the Cathaysia block in southeastern China (Figure 1) consists of Precambrian basement and an overlying Phanerozoic igneous and sedimentary sequence (Xu et al., 2016). Paleoproterozoic and Mesoproterozoic granitic rocks within this block were given ages of 1890–1800 and 1450–1430 Ma (Li et al., 2008; Yu et al., 2009), respectively. Neoproterozoic rocks with an age peak at circa 967 Ma (Figure 7D) occur widely throughout the block. Voluminous Paleozoic to Mesozoic granitic plutons that are related to tectonic–thermal events in the southern China block yielded major age peaks ranging from 450 to 130 Ma (Figure 7D). The Qiangtang block in the northern Tibetan Plateau is bounded by the Jinsha suture to the north and the Bangong–Nujiang suture to the south (Figure 1A). This block mainly consists of sub-Jurassic strata and metamorphic rocks in the central segment and Jurassic sedimentary rocks along the northern and southern margins. The lower Paleozoic and Mesozoic magmatic and metamorphic rocks within the block were dated at 470–430 and 240–200 Ma (Zhai et al., 2011), respectively. A major young Indosinian peak was observed at circa 221 Ma, with five subordinate age peaks observed at circa 440, 639, 972, 1938, and 2505 Ma (Figure 7E). The Songpan–Garze block, which formed during the closure of the paleo-Tethys Ocean, is located in the eastern Tibetan Plateau (Figure 1A) (Bruguier et al., 1997). This block is bounded by the Yangtze, North China, and Qiangtang blocks and is characterized by marine Triassic flysch deposits and widespread granitic rocks. Previous studies (Weislogel et al., 2006; Enkelmann et al., 2007; Ding et al., 2013) showed a wide range of U-Pb ages in this block, with four major age peaks of circa 245, 448, 781, and 1852 Ma (Figure 7F).

Source of Detrital Zircons

The age populations for the samples in this study were compared with the age signatures of the aforementioned potential sediment sources. In these samples (Figures 5 and 6), detrital zircons with ages of circa 2200–2800 Ma are interpreted as having been derived from the southern Yangtze block (Zheng et al., 2006) or possibly recycled from Paleozoic sedimentary rocks in the eastern Indochina block (Wang et al., 2016b). The Proterozoic ages of circa 1700–2100 Ma are consistent with the tectonic–magmatic event in the Yangtze block. However, significant age populations between 1852 and 1938 Ma could also be derived from the Cathaysia, Qiangtang, and Songpan–Garze blocks (Figure 7D–F). Neoproterozoic zircons with age peak at circa 865 Ma are likely from a distinctive signature in the Yangtze block and are absent or only account for a small fraction in other source terranes (Li et al., 2003; Hoang et al., 2009). The Neoproterozoic ages between 900 and 1000 Ma could have been derived from the hinterland of Cathaysia, Qingtang (Figure 7D, E), or eastern Indochina (Jonell et al., 2017). The Paleozoic zircons with U-Pb ages between 420 and 480 Ma correspond to widespread Paleozoic magmatic and metamorphism in eastern Asia and elsewhere in Gondwana (Li et al., 2010); these zircons could have been derived from the Yangtze, Cathaysia, or Indochina blocks (Figure 7). Mesozoic-aged zircon populations dominated the provenance record (Figures 5 and 6), indicating a significant provenance that was associated with a Triassic thermo-tectonic event (Indosinian orogeny) in East Asia. These ages, which ranged from 280 to 230 Ma, were ubiquitous for all the source terranes (Figure 7) and had limited potential as a decisive source indicator. The Cretaceous zircons from circa 100 Ma are probably from the distinctive sources in Hainan (Figure 7B), so they could have been derived from different drainage systems in western Hainan (Cao et al., 2015; Wang et al., 2015b). Cenozoic zircon grains in these samples (e.g., L11-1, 30 Ma) are most likely from a distinct source along the RRFZ in the southern Yangtze block (Zhang and Schärer, 1999; Clift et al., 2006a).

Compared to these potential source terranes, 4 of the 10 Cenozoic samples from group 2 (i.e., L11-5, L15-1, L15-3, and L26-5) contained high proportions of Cretaceous (ca. 98 Ma, 35.2% in total) and Triassic (ca. 240 Ma, 51.5% in total) zircons, with a limited number of ages older than 450 Ma, which suggests that Hainan was the main source region for the Yingdong slope during the Miocene–Pliocene (Yan et al., 2011; Wang et al., 2014). In addition, the zircon grains from these samples were angular without rounded corners (e.g., L15-1, L26-5) (Figure 4), which are consistent with a proximal source. This interpretation is further supported by detrital zircon U-Pb geochronological studies of modern drainage systems in Hainan (Cao et al., 2015; Wang et al., 2015b) (Figure 7H).

The zircon age populations of six samples assigned to group 1 (i.e., L11-1, L11-2, L11-4, L11-12, L35-3, and L35-4) were relatively complex and significantly distinct from the group 2 samples (Figures 5 and 6). Some zircon grains in these samples were rounded to subrounded, indicating that they were probably transported a long distance or multicycle detrital zircon that were eroded from the sedimentary rocks around the basin (Usuki et al., 2013). The age spectra of these samples were broadly similar, with age peaks ranging from the Archean to Cenozoic (Figures 5 and 6), which is consistent with the polyphase evolution of the Yangtze block (Wang et al., 2010). The abundant Neoproterozoic zircons with ages of circa 730–760 and 940–970 Ma were interpreted to have been originally derived from the southern Yangtze block. However, a recent study by Jonell et al. (2017) showed that these age populations could also be found in central Vietnam, although they were still presumed to have eroded from the Yangtze block in the distant geological past. A source from the Red River is also supported by scattered Cenozoic zircons, which were likely derived from the RFFZ in some samples, such as L11-1 and L35-4 (Table S1, supplementary material available as AAPG Datashare 108 at www.aapg.org/datashare). The lower Paleozoic (ca. 420–445 Ma) and Neoarchean to Paleoproterozoic zircons (ca. 2420–2530 Ma) were presumably shed from the southern Yangtze block or the Truong Son belt in the eastern Indochina block. Nevertheless, samples L11-2 and L11-4 showed several distinct characteristics between the two groups of sedimentary rocks (Figure 5B, C): these samples had identical components to those of the samples in group 1 but also contained Cretaceous zircons (ca. 100 and 104 Ma, respectively), similar to the samples from Hainan. These two samples probably had mixed sources with sediments from both the Yangtze block and Hainan.

Detritus in group 1 samples might have also been derived from other sources, including the Songpan–Garze, Qiangtang, and the hinterland of the Cathaysia blocks, and delivered by the Red River (Figure 1) (Clift et al., 2006a; Hoang et al., 2009). The Cathaysia block (Figure 7D) had a more complicated age distribution pattern and was largely characterized by an age population that was centered at circa 133 Ma, with distinct age peaks at circa 1437 Ma. Such grains were rare in the studied samples, indicating that the hinterland of the Cathaysia block was probably not the main source terrane for the eastern Y-SH Basin. Although samples L35-4 and L35-3 had similar Cretaceous peaks (144 and 127 Ma, respectively), they should have also been derived from the Hainan at the southern end of the Cathaysia block (Cao et al., 2015; Wang et al., 2015b). The relatively limited zircon grain ages that ranged from 220 to 200 Ma could have come from the Qiangtang block (Van Hoang et al., 2009), but the absence of 500–700 Ma zircons makes this a less likely source. The Songpan–Garze block exhibits a wide range of zircon U-Pb ages, with a large peak at 1852 Ma, which is different than the southern Yangtze block (Figure 7F). Although the age population at 1700–2000 Ma was observed in the samples (such as L11-1 and L11-4), this range probably represents input from the Yangtze and Songpan–Garze blocks. Hoang et al. (2009) also proposed that this distinctive age population in the modern Red River should have been reworked via sedimentary basins in the upper Red River. Therefore, we cannot preclude additional input from the Songpan–Garze block.

Multidimensional scaling (MDS) plots (Figure 8) were used in this study to assess the relative dissimilarities of samples (Vermeesch, 2013, 2014a, b, 2016). Generally, samples with similar age compositions were grouped in the MDS plots and separated if they were dissimilar. In the metric MDS plots of zircon U-Pb data, these samples showed a distinct affinity with the potential source terranes (Figure 8A) and the drainage systems around the Y-SH Basin (Figure 8B). Notably, both eastern Indochina and the drainage systems in central Vietnam plotted far from these samples, distinguishing a source from the west and suggesting a minor contribution from the Indochina block. The samples along the eastern side of the basin, such as L11-5 and L26-5, showed a greater affinity for the Hainan area as defined by the zircon ages from the bedrocks and modern rivers (Figure 8). By contrast, L11-2 and L11-4 were more similar to the eastern Indochina provenance. This correlation probably occurred because these two samples were primarily sourced from central Vietnam (eastern Indochina); alternatively, the sediments from these two samples were derived from a mixed-source area, producing more similar age spectra to that of eastern Indochina. Many of the samples showed a stronger affinity to the southern Yangtze block rather than the Indochina block and reflected an important contribution from this source terrane. In addition to the southern Yangtze block, samples L262-1 and L11-1 were associated with sources that were related to the Cathaysia, Qiangtang, and Songpan–Garze blocks, which plotted far from most samples and were clearly distinguishable based on their relative clustering (Figure 8A), indicating the possible influences

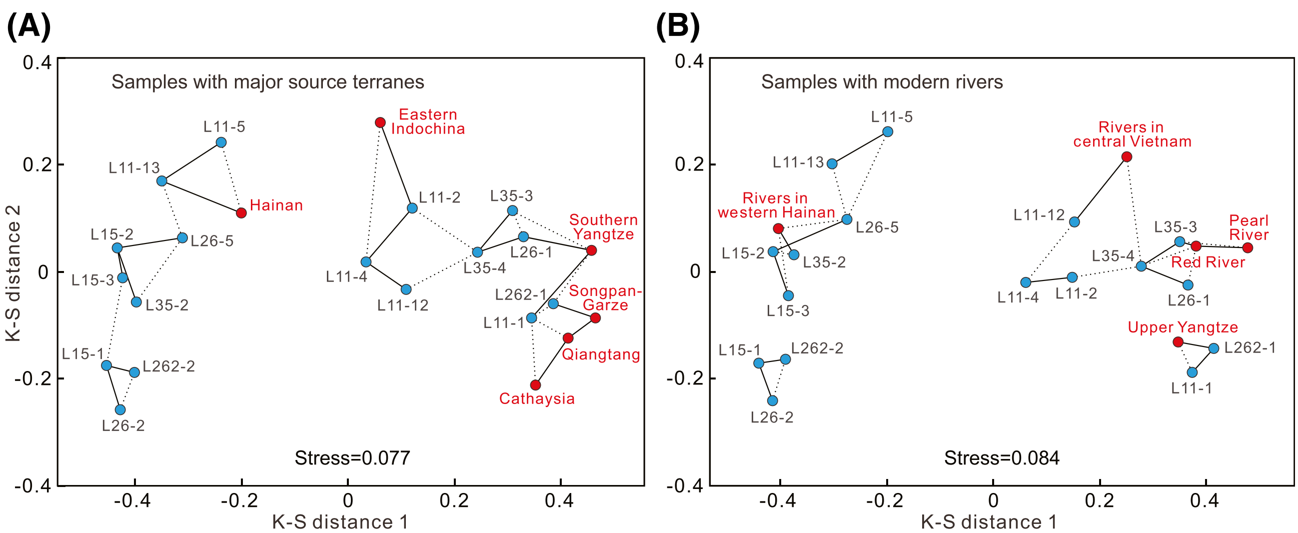

Figure 8. Metric multidimensional scaling plots based on the Kolmogorov–Smirnov (K-S) distances between samples and potential source terranes (A) and drainage systems around the Yinggehai–Song Hong Basin (B) based on the data in this paper and associated studies that were discussed in the text.

of these sources. However, some overlapping age populations existed between the Yangtze block and these three source terranes (Figure 7D–F), making this relationship difficult to distinguish within the MDS plots.

In summary, detrital zircon data from the Yingdong slope showed that the sedimentary rocks were derived from multiple sources. A comparison of the age populations with the potential source terranes indicate that the Red River and Hainan were key factors in the sedimentary provenance contributions to the eastern Y-SH Basin, and additional minor sources likely shed westwards from central Vietnam (eastern Indochina block) and possibly the Songpan–Garze block. In contrast, the Qiangtang and the hinterland of the Cathaysia blocks do not appear to have been source terranes but could have provided limited sedimentary contributions to the eastern Y-SH Basin.

Variations and Similarities between Samples

Detrital zircons from the eastern Y-SH Basin samples give U-Pb ages that ranged from 3078 to 30 Ma, revealing input from multicomponent sources. The possible provenance and transport pathways that would produce this mixture are shown in Figure 9, where the example shows detritus arriving in the Yingdong slope mainly by long-distance transport from the Red River to the northwest and by short-distance transport from Hainan. The Red River was the main source because of its large flux and transport capacity (Wang et al., 2015a). The modern Red River drains an area of 160,000 km^2 (62,000 mi^2) and flows approximately 1200 km (~750 mi) from the mountains of Yunnan Province, with a total sediment and water discharge of $100–130 \times 10^6$ t/yr ($98–128 \times 10^9$ lb/yr) and 120 km^3/yr (28.8 mi^3/yr), respectively (Milliman et al., 1995; Pruszak et al., 2002).

No clear correlation exists between the current sample locations and the source terranes for strata above the lower Miocene Sanya Formation, suggesting that the source remained broadly diverse at least for the sampled succession (Sircombe et al., 2001; Benyon et al., 2016). Notwithstanding, the detrital zircon ages also indicated several changes in the dominant source terranes over time. Borehole L15 shows similar age spectra among different strata and reveals a relatively stable source system since the early Miocene (ca. 17.5 Ma) (Figure 5G–I). The Red River detritus was not significant at this location, as indicated by the absence or scarcity of Neoproterozoic and Paleoproterozoic zircon ages (>600 Ma). The L15 location, therefore, maintained a stable source supply only from Hainan. The age spectra of the Meishan Formation (ca. 15.5–13.8 Ma) for borehole L35 give bimodal age populations, which change from the upper Yinggehai (ca. 2.4–1.8 Ma) and Ledong (ca. 1.8 Ma–present) formations. The strata with multipeak zircon age distributions (Figure 6F–H) suggest mixed provenance from the Hainan and Red River sources.

The systemic analyses of L26 and L11 provide an example of the provenance variations in the strata (Figures 5 and 6). Changes in the zircon age spectra in borehole L26 (Figure 6A–E) indicate that Red River sources dominated during the early-middle Miocene (ca. 15.5–13.8 Ma) and late Miocene (ca. 8.2–5.5 Ma). Whereas, the detrital zircon populations from the other strata, which contained moderate to high concentrations of Triassic and Cretaceous grains, are consistent with the local bedrock in Hainan (Figure 7B). The zircon age spectra in borehole L11 showed that the sedimentary source patterns intermittently changed over time (Figure 5A–F). The middle–upper Miocene (13.8–5.5 Ma) exhibited bimodal age spectra and consisted of 98–101 and 236–243 Ma components, indicating that they were locally derived from Hainan, with smaller amounts of detritus from the Red River during the late Miocene (10.5–8.2 Ma). In contrast, the age spectra became more complicated during the Pliocene (5.5–1.8 Ma) with the addition of Paleoproterozoic, Neoproterozoic, and lower Paleozoic ages, indicating that the detritus was derived from both the Red River and Hainan source regions.

Provenance Evolution and Contributions

The possible sediment transportation directions of sediments throughout the Y-SH Basin based on the previously published data and the detrital zircon U-Pb geochronological data analysis in this study is shown in Figure 10. Comparing the zircon age spectra for the coeval strata of boreholes across the basin suggests systematic changes in sediment supply for different parts of the basin through time. The

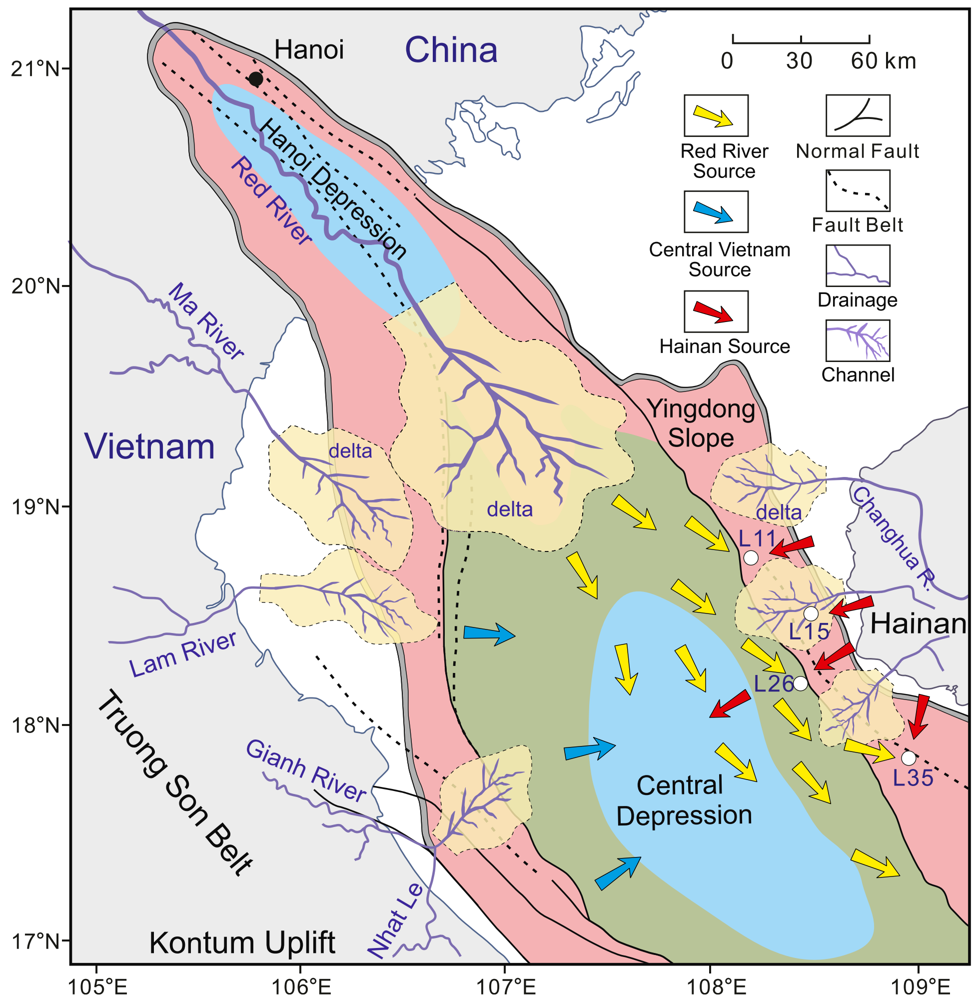

Figure 9. Hypothesis that depicts the sediment transportation pathways of the eastern Yinggehai–Song Hong Basin. The modern drainage systems were adopted from Sun et al. (2014). R. = River.

provenance evolution of the Y-SH Basin can be summarized as follows.

From the late Oligocene to early Miocene (ca. 30.0–15.5 Ma), the major depocenter was located in the northwestern Y-SH Basin and gradually migrated southeastward to the Central depression because of the left-lateral slip movement of the RRFZ (Figure 10A, B). The populations of detrital zircons from the upper Oligocene indicate that the sediments in the eastern and southeastern basin were mainly from the nearby Hainan area (Yan et al., 2011). The influence of Red River detritus could not be evaluated for upper Oligocene strata because of the limited sample and geochronological data from the boreholes. Hainan was also an important source of detritus to the eastern Y-SH Basin during the early Miocene (Figure 10B). Red River detritus has been identified in the northern basin at the same time (Wang et al., 2016c).

During the middle Miocene (ca. 15.5–10.5 Ma), both Hainan and the Red River were the major source terranes for the Y-SH Basin (Figure 10C, D). Slip reversal on the RRFZ affected basin sedimentation by causing the depocenters to move from the southern area of the basin to the center. In the eastern basin, with the exception of sample L26-1, the wide detrital zircon age ranges from 2728 to 103 Ma were similar to sources within the southern Yangtze block, implying long-distance transport from the Red River (Wang et al., 2016a). The remaining samples in this study all originated from Hainan through different drainage systems (Cao et al., 2015; Wang et al., 2015b), including the Changhua River (Figure 9). This suggests that Hainan

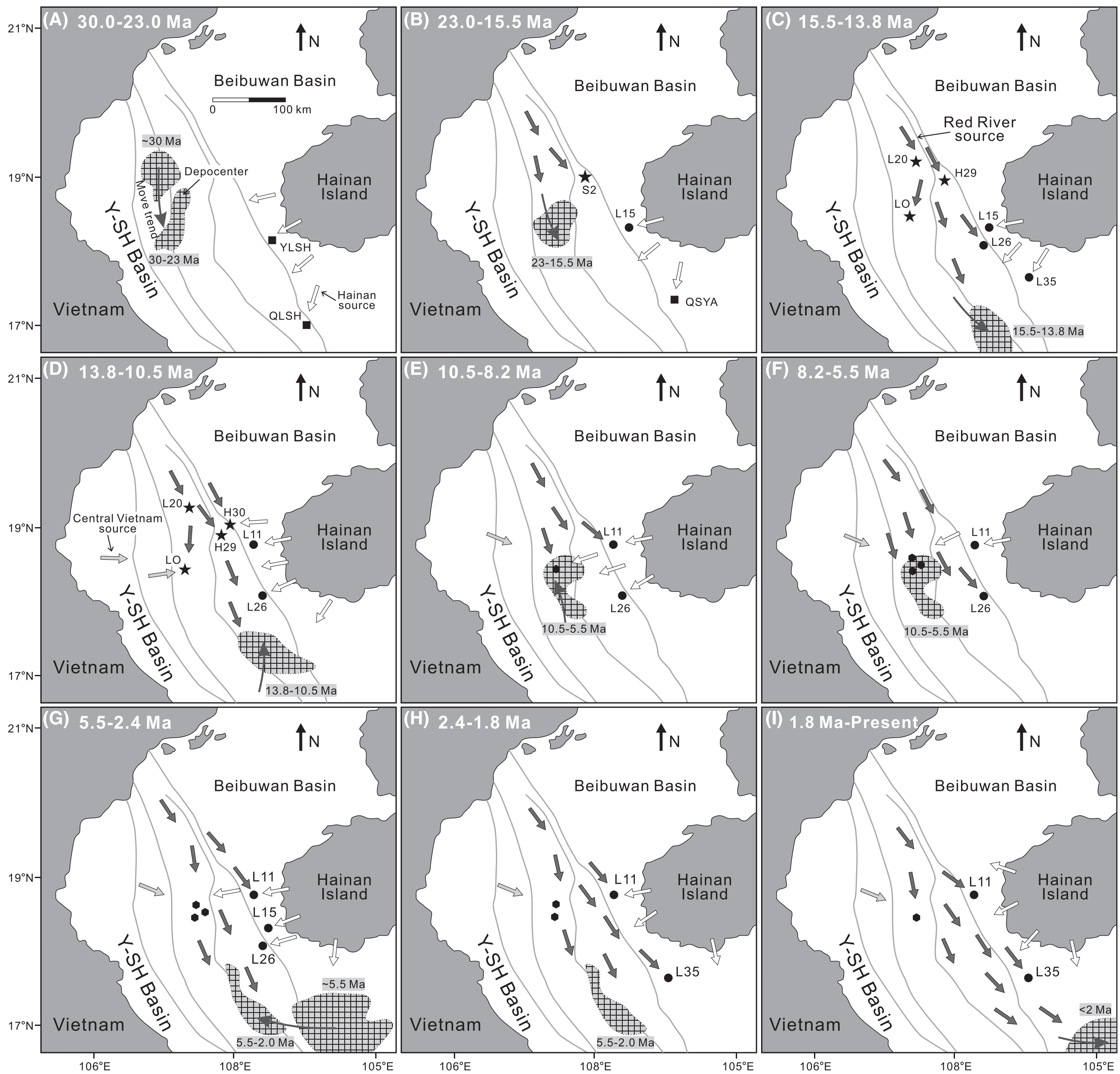

Figure 10. (A–I) Possible provenance evolution of the sedimentary rocks in the eastern Yinggehai–Song Hong (Y-SH) Basin since the late Oligocene. The depocenters are from Sun et al. (2003) and Zhu et al. (2009). H29, H30, L11, L15, L20, L26, L35 are boreholes. QLSH, QMSH, QSYA, and S2 are the sample names. Samples from borehole H29, H30, LO and L20 are from Wang et al., (2016a).

was a major source for eastern Y-SH Basin sediment. By contrast, the northwestern basin was dominated by the Red River source in the middle Miocene (Figure 10C, D).

During the late Miocene (10.5–5.5 Ma), the depocenters migrated to the center of the basin because of fault reversal (Figure 10E, F). Discrepant U-Pb age patterns between the lower and upper Huangliu Formation at boreholes L11 and L26 probably indicate intraformational provenance variations in the study region. Sediments that were transported southeastward by the Red River could have reached the location of borehole L26 in the basin (Figure 10F), likely indicating the long submarine transport of detrital material from the Red River or recycling of clastic sedimentary rocks around the basin. The sedimentary rocks in the central basin mainly originated from the Red River during the late Miocene, with minor contributions from central Vietnam and Hainan.

From the Pliocene to Quaternary (since 5.5 Ma), the major depocenters migrated to the southeast, eventually reaching the neighboring Qiongdongnan Basin. At this time, the provenance of the eastern Y-SH Basin shifted from Hainan to the Red River (Figure 10G–I). Detritus from the Red River rapidly increased over this interval and became the main source to the southeastern basin, reaching the location of borehole L35 in the south of Hainan by circa 2 Ma (Figure 10H–I).

Generally, the Paleozoic and Neoproterozoic detrital zircons gradually increase in population from the upper Oligocene Lingshui Formation to Quaternary Ledong Formation (since ca. 30 Ma) (Figures 5 and 6). Variations in the dominant detrital zircon populations within the vertical stratigraphic successions clearly show increasing contributions from the Red River since at least the middle Miocene (Figure 10) as the result of the expansion of the delta in the northern Y-SH Basin. Coverage area of the Red River Delta in the northern region of the basin has been extending since the early Miocene (Xie, 2009), and sediments have since been transported over long distances (Figure 9). Progradation into the central and southeastern area of the basin is consistent with the evolution of the depocenters over time. The relatively stationary depocenters during the Oligocene–early Miocene (30–15.5 Ma) (Figure 10A, B) trapped most of the Red River detritus in the northern and central basin (Hoang et al., 2010b). Migration of the primary depocenters back to the northwest between 15.5 and 5.5 Ma was probably because of motion on the RRFZ more than delta growth (Figure 10C–F). After the Pliocene (ca. 5.5 Ma), depocenter migration to the northeastern Y-SH Basin resulted in sediment overspilling to the east into the Qiongdongnan Basin (Figure 10G–I).

The intensification of the East Asian monsoon could have been another important factor that controlled continental weathering-erosion processes and affected the composition and volume of sediments from the Red River (Wan et al., 2006; Hoang et al., 2010b). The sediment provenance was undeniably influenced by the regional surface uplift and associated climate changes in East Asia (An et al., 2001; Clift et al., 2008; Li et al., 2014). The stratigraphic record and thermochronometric data indicated that intensified erosion began and reached a peak at circa 15 Ma and lasted until 10.5 Ma (Clift et al., 2008). This timing is consistent with the increase in sediment accumulation rates in the Y-SH Basin. Hoang et al. (2010b) suggested a relationship between the shift to more physical erosion and increasing sedimentation rates in Southeast Asia after circa 15.5 Ma. Changes in the Y-SH Basin sediment flux since the middle Miocene (ca. 16 Ma), especially the apparent increase in sediment accumulation rates between 15.5 and 10 Ma (Clift and Sun, 2006; Hoang et al., 2010b), caused the accumulation of deltaic material and progradation to the central basin. The uplift of the Tibetan Plateau (Schoenbohm et al., 2006) and the associated monsoon governed the regional erosion and sedimentation rates (Zhang et al., 2001) and increased the volume, changed the composition, and affected the transportation distance of sediments that were delivered from the Red River to the Y-SH Basin (Hoang et al., 2010a). Thus, we attribute the increased source contribution from the Red River since the middle Miocene to the progradation of the delta and possible influence of regional surface uplift and associated climate changes in East Asia.

Constraining the Drainage Capture of the Red River

Changes in the regional drainage that were associated with the Red River capture inevitably affected the volumes and compositions of the sediments that reached the deltas in the South China Sea; therefore, we could use the sediment record from the Y-SH Basin to better understand the evolution of the Red River. Compared to other potential source terranes, the Qiangtang block in central Tibet is largely characterized by Triassic zircon grains that concentrated at circa 221 Ma (Roger et al., 2003), along with a Paleoproterozoic age peak at circa 1938 Ma and a distinct population of 500–700-Ma zircons (Figure 7E). In contrast, the Songpan–Garze block shows a Neoproterozoic age peak of circa 781 Ma and a higher proportion of Paleoproterozoic populations at circa 1852 Ma (Figure 7F). If the upper Yangtze was once connected with the paleo–Red River, then these distinct age populations from the Qiangtang and Songpan–Garze blocks should be detected in samples from the Y-SH Basin (Figure 11). Such age peaks (especially zircon ages of 500–650 and 1800–2000 Ma) were not observed or did not comprise a significant part of the total age spectrum in the Y-SH Basin (Figures 5 and 6), suggesting that the sediments were not derived from the Qiangtang block. We could not evaluate contributions from the Songpan–Garze block because of the age overlap with the southern Yangtze block (Figure 7A). These observations preclude much sediment flux from the Qiangtang block and probably suggest that there was no connection between the Red River and upper Yangtze River if most of the sediments in the river were derived from the Qiangtang block as it is today. Although samples L11-1 and L262-1 showed an affinity with the upper Yangtze River in the MDS plot (Figure 8B), it is not unique. The sedimentary rocks in the Y-SH Basin do not yield a zircon age peak of circa 1437 Ma, which is considered an important signature for the Cathaysia block (Figure 7D) (Hoang et al., 2009), negating the hypothesis that the Red River was once connected to the Pearl River (Figure 11). In addition, sample L35-3 shows a weak correlation with the Pearl River but a close correlation to the Red River (Figure 8B). This does not mean that a part of the sediments was derived directly from the Pearl River. Conversely, it was caused by the overlapping age populations that existed between these two rivers (Figure 7).

The new and previously published detrital zircon data with a different geological age from the early Miocene to Quaternary with a Red River source are plotted in Figure 12A to further understand the provenance evolution of the Red River sediment. Statistical zircon data from the Archean to Carboniferous (ages older than 300 Ma) are presented in Figure 12B. This was done to avoid the Hainan source with a high proportion of Permian to Cretaceous zircons. The detrital zircon data show no obvious anomalies among most of the samples giving similar age characteristics to the modern Red River sediment. This suggests that the Red River provenance has been relatively stable since at least the early Miocene (ca. 23 Ma) and does not support large-scale drainage capture of the Red River since the Miocene. This conclusion is also corroborated by geochemical evidence from sedimentary rocks in the Y-SH Basin, which shows no change in composition since the late Oligocene (Zhao et al., 2015a).

In the detrital zircon signatures of the strata, there are some minor changes (Figure 12B). The lower Huangliu Formation gives a smaller proportion of lower Paleozoic zircons than all other formations. This could be explained by additional flux of Paleozoic zircons from Song Lo when it joined the Red River after circa 9 Ma (Clift et al., 2008), delivering more detritus from the Cathaysia and Yangtze blocks. In addition, the Sanya and lower Meishan Formations (23.0–13.8 Ma) contained relatively few Mesoproterozoic grains (Figure 12B), whereas the upper Yinggehai Formation (2.4–1.8 Ma) had a higher content of Paleoproterozoic zircons, similar to those

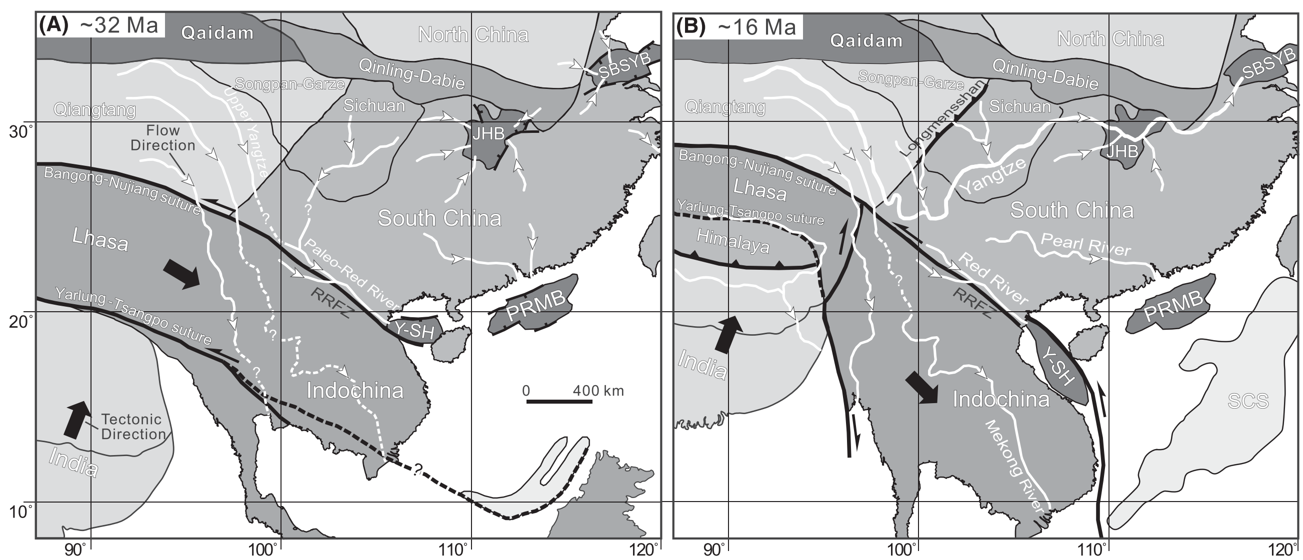

Figure 11. Simplified maps that show the evolution of drainage systems in East Asia at (A) 32 Ma and (B) 16 Ma, modified after Zheng et al. (2013). JHB = Jianghan Basin; PRMB = Pearl River Mouth Basin; RRFZ = Red River fault zone; SBSYB = Subei–South Yellow Sea Basin; SCS = South China Sea; Y-SH = Yinggehai–Song Hong.

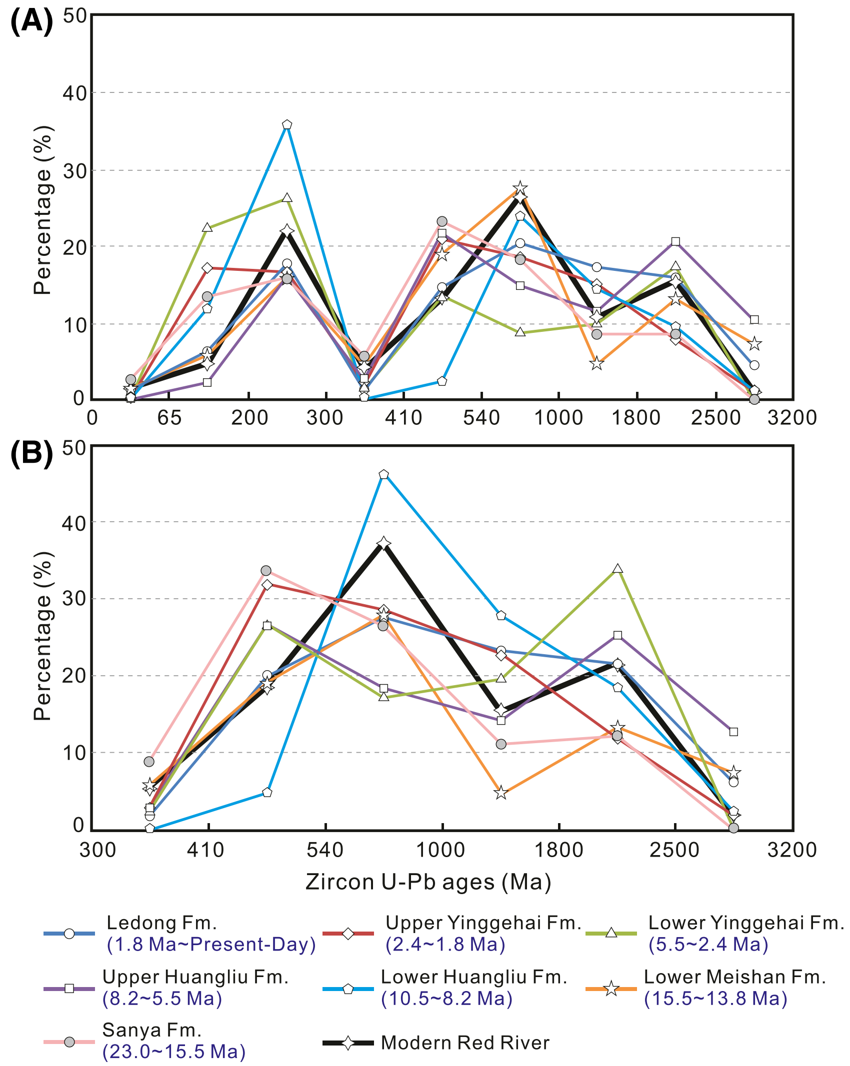

Figure 12. Detrital zircon age distribution of different strata in the eastern Yinggehai–Song Hong Basin (sourced from the Red River) based on geological time statistics from (A) the Archean to Cenozoic and (B) the Archean to Carboniferous (ages older than 300 Ma). Fm. = Formation.

with a Red River provenance, suggesting slight provenance changes among the sedimentary periods since the early Miocene.

Although we cannot exactly determine the time of drainage capture in this study, the similarity between the borehole zircon ages and the U-Pb ages of zircon in the modern Red River source suggests that no significant provenance changes occurred in the Red River area since at least the early Miocene (Figure 12). Characterization of the current detrital zircon record does not support a connection between the Red and Yangtze Rivers in the Neogene. If large-scale drainage reorganization of the Red River did occur, it should have been before the early Miocene (ca. 23 Ma).

CONCLUSIONS

The new data set of detrital zircon ages that was provided by this work improved our understanding of the provenance for the eastern Y-SH Basin. The synthesis of new and published detrital zircon U-Pb ages from the Yingdong slope demonstrate spatial and temporal changes in sediment provenance, reflecting the evolution of sediment dispersal patterns from the early Miocene to Quaternary. The measured zircon age distributions show that approximately half of the age components in the Cenozoic sedimentary rocks could be attributed to a local source that was mainly derived from Hainan. The other component with zircon U-Pb ages that range from Archean to Cenozoic with multipeak characteristics are consistent with detritus originally derived from the southern Yangtze block and transported along the Red River. A comparison of these age populations with potential source terranes indicated that both the Red River and Hainan were key factors in contributing to the eastern Y-SH Basin, with additional minor sediment contributions from central Vietnam (eastern Indochina block) and possibly the Songpan–Garze block. The local source in Hainan significantly influenced the eastern Y-SH Basin before the middle Miocene, suggesting a stable provenance from Hainan during deposition. The sediment supply from the southern Yangtze block through the Red River gradually increased since the middle Miocene, becoming the dominant source thereafter. The increased input of Red River detritus suggests the progradation of the river delta from the north of the basin and possibly the regional surface uplift and associated climate changes in East Asia. The Red River sources have not changed considerably since at least the early Miocene, suggesting that any Red River capture should have occurred before the early Miocene (ca. 23 Ma).

REFERENCES CITED

An, Z., J. E. Kutzbach, W. L. Prell, and S. C. Porter, 2001, Evolution of Asian monsoons and phased uplift of the Himalaya-Tibetan plateau since Late Miocene times: Nature, v. 411, no. 6833, p. 62–66, doi:10.1038/35075035.

Andersen, T., 2002, Correction of common lead in U-Pb analyses that do not report ^{204}Pb: Chemical Geology, v. 192, no. 1–2, p. 59–79, doi:10.1016/S0009-2541(02)00195-X.

Benyon, C., A. L. Leier, D. A. Leckie, S. M. Hubbard, and G. E. Gehrels, 2016, Sandstone provenance and insights into the paleogeography of the McMurray Formation from detrital zircon geochronology, Athabasca Oil Sands, Canada: AAPG Bulletin, v. 100, no. 2, p. 269–287, doi:10.1306/10191515029.

Bracciali, L., Y. Najman, R. R. Parrish, S. H. Akhter, and I. Millar, 2015, The Brahmaputra tale of tectonics and erosion: Early Miocene river capture in the Eastern Himalaya: Earth and Planetary Science Letters, v. 415, p. 25–37, doi:10.1016/j.epsl.2015.01.022.

Brookfield, M. E., 1998, The evolution of the great river systems of southern Asia during the Cenozoic India-Asia collision: Rivers draining southwards: Geomorphology, v. 22, no. 3–4, p. 285–312, doi:10.1016/S0169-555X(97)00082-2.

Bruguier, O., J. R. Lancelot, and J. Malavieille, 1997, U–Pb dating on single detrital zircon grains from the Triassic Songpan–Garze flysch (Central China): Provenance and tectonic correlations: Earth and Planetary Science Letters, v. 152, no. 1–4, p. 217–231, doi:10.1016/S0012-821X(97)00138-6.

Cao, L., T. Jiang, Z. Wang, Y. Zhang, and H. Sun, 2015, Provenance of Upper Miocene sediments in the Yinggehai and Qiongdongnan basins, northwestern South China Sea: Evidence from REE, heavy minerals and zircon U-Pb ages: Marine Geology, v. 361, p. 136–146, doi:10.1016/j.margeo.2015.01.007.

Carter, A., D. Roques, C. Bristow, and P. Kinny, 2001, Understanding Mesozoic accretion in Southeast Asia: Significance of Triassic thermotectonism (Indosinian orogeny) in Vietnam: Geology, v. 29, no. 3, p. 211–214, doi:10.1130/0091-7613(2001)029<0211:UMAISA>2.0.CO;2.

Cawood, P. A., and A. A. Nemchin, 2000, Provenance record of a rift basin: U/Pb ages of detrital zircons from the Perth Basin, Western Australia: Sedimentary Geology, v. 134, no. 3–4, p. 209–234, doi:10.1016/S0037-0738(00)00044-0.

Cawood, P. A., A. A. Nemchin, M. Freeman, and K. Sircombe, 2003, Linking source and sedimentary basin: Detrital zircon record of sediment flux along a modern river system and implications for provenance studies: Earth and Planetary Science Letters, v. 210, no. 1–2, p. 259–268, doi:10.1016/S0012-821X(03)00122-5.

Cawood, P. A., A. A. Nemchin, R. A. Strachan, P. D. Kinny, and S. Loewy, 2004, Laurentian provenance and an intracratonic tectonic setting for the Moine Supergroup, Scotland, constrained by detrital zircons from the Loch Eil and Glen Urquhart successions: Journal of the Geological Society, v. 161, no. 5, p. 861–874, doi:10.1144/16-764903-117.

Chen, Y., M. Yan, X. Fang, C. Song, W. Zhang, J. Zan, Z. Zhang, B. Li, Y. Yang, and D. Zhang, 2017, Detrital zircon U-Pb geochronological and sedimentological study of the Simao Basin, Yunnan: Implications for the Early Cenozoic evolution of the Red River: Earth and Planetary Science Letters, v. 476, p. 22–33, doi:10.1016/j.epsl.2017.07.025.

Chen, Z., W. Lin, M. Faure, C. Lepvrier, N. Van Vuong, and V. Van Tich, 2014, Geochronology and isotope analysis of the Late Paleozoic to Mesozoic granitoids from northeastern Vietnam and implications for the evolution of the South China block: Journal of Asian Earth Sciences, v. 86, p. 131–150, doi:10.1016/j.jseaes.2013.07.039.

Clark, M. K., L. M. Schoenbohm, L. H. Royden, K. X. Whipple, B. C. Burchfiel, X. Zhang, W. Tang, E. Wang, and L. Chen, 2004, Surface uplift, tectonics, and erosion of eastern Tibet from large-scale drainage patterns: Tectonics, v. 23, no. 1, 21 p., doi:10.1029/2002TC001402.

Clift, P. D., 2006, Controls on the erosion of Cenozoic Asia and the flux of clastic sediment to the ocean: Earth and Planetary Science Letters, v. 241, no. 3–4, p. 571–580, doi:10.1016/j.epsl.2005.11.028.

Clift, P. D., J. Blusztajn, and A. D. Nguyen, 2006b, Large-scale drainage capture and surface uplift in eastern

Tibet-SW China before 24 Ma inferred from sediments of the Hanoi Basin, Vietnam: Geophysical Research Letters, v. 33, no. 19, 5 p., doi:10.1029/2006GL027772.
Clift, P. D., A. Carter, I. H. Campbell, M. S. Pringle, N. Van Lap, C. M. Allen, K. V. Hodges, and M. T. Tan, 2006a, Thermochronology of mineral grains in the Red and Mekong Rivers, Vietnam: Provenance and exhumation implications for Southeast Asia: Geochemistry Geophysics Geosystems, v. 7, no. 10, 28 p., doi:10.1029/2006GC001336.
Clift, P. D., A. Carter, L. Giosan, J. Durcan, G. A. Y. Duller, M. G. Macklin, A. Alizai et al., 2012, U-Pb zircon dating evidence for a Pleistocene Sarasvati River and capture of the Yamuna River: Geology, v. 40, no. 3, p. 211–214, doi:10.1130/G32840.1.
Clift, P. D., K. V. Hodges, D. Heslop, R. Hannigan, H. Van Long, and G. Calves, 2008, Correlation of Himalayan exhumation rates and Asian monsoon intensity: Nature Geoscience, v. 1, no. 12, p. 875–880, doi:10.1038/ngeo351.
Clift, P. D., J. I. Lee, M. K. Clark, and J. Blusztajn, 2002, Erosional response of South China to arc rifting and monsoonal strengthening; a record from the South China Sea: Marine Geology, v. 184, no. 3–4, p. 207–226, doi:10.1016/S0025-3227(01)00301-2.
Clift, P. D., and Z. Sun, 2006, The sedimentary and tectonic evolution of the Yinggehai-Song Hong basin and the southern Hainan margin, South China Sea: Implications for Tibetan uplift and monsoon intensification: Journal of Geophysical Research. Solid Earth, v. 111, 28 p., doi:10.1029/2005JB004048.
DeCelles, P. G., G. E. Gehrels, Y. Najman, A. J. Martin, A. Carter, and E. Garzanti, 2004, Detrital geochronology and geochemistry of Cretaceous–Early Miocene strata of Nepal: Implications for timing and diachroneity of initial Himalayan orogenesis: Earth and Planetary Science Letters, v. 227, no. 3–4, p. 313–330, doi:10.1016/j.epsl.2004.08.019.
Ding, L., D. Yang, F. L. Cai, A. Pullen, P. Kapp, G. E. Gehrels, L. Y. Zhang et al., 2013, Provenance analysis of the Mesozoic Hoh-Xil-Songpan-Ganzi turbidites in northern Tibet: Implications for the tectonic evolution of the eastern Paleo-Tethys Ocean: Tectonics, v. 32, no. 1, p. 34–48, doi:10.1002/tect.20013.
Dong, C., C. Li, Y. Wan, W. Wang, Y. Wu, H. Xie, and D. Liu, 2011, Detrital zircon age model of Ordovician Wenquan quartzite south of Lungmuco-Shuanghu Suture in the Qiangtang area, Tibet: Constraint on tectonic affinity and source regions: Science China Earth Sciences, v. 54, no. 7, p. 1034–1042, doi:10.1007/s11430-010-4166-x.
Duan, W., and Y. Huang, 1991, Tertiary calcareous nannofossil biostratigraphy in the north part of the South China Sea (English edition): Acta Geologica Sinica, v. 4, p. 321–338, doi:10.1111/j.1755-6724.1991.mp4003008.x.
Enkelmann, E., A. Weislogel, L. Ratschbacher, E. Eide, A. Renno, and J. Wooden, 2007, How was the Triassic Songpan-Ganzi basin filled? A provenance study: Tectonics, v. 26, no. 4, 24 p., doi:10.1029/2006TC002078.
Fontanelli, P. D. R., L. F. De Ros, and M. V. D. Remus, 2009, Provenance of deep-water reservoir sandstones from the Jubarte oil field, Campos Basin, Eastern Brazilian Margin: Marine and Petroleum Geology, v. 26, no. 7, p. 1274–1298, doi:10.1016/j.marpetgeo.2008.09.010.
Gilley, L. D., T. M. Harrison, P. H. Leloup, F. J. Ryerson, O. M. Lovera, and J. H. Wang, 2003, Direct dating of left-lateral deformation along the Red River shear zone, China and Vietnam: Journal of Geophysical Research. Solid Earth, v. 108, 21 p., doi:10.1029/2001JB001726.
Gong, Z., S. Li, T. Xie, Q. Zhang, S. Xu, K. Xia, J. Yang, Y. Sun, and L. Liu, 1997, Continental margin basin analysis and hydrocarbon accumulation of the northern South China Sea: Beijing, China, Science Press, p. 29–86.
Guo, L., Z. Zhong, L. Wang, Y. S. Shi, H. Li, and S. W. Liu, 2001, Regional tectonic evolution around Yinggehai basin of South China Sea: Geological Journal of China Universities, v. 7, p. 1–12.
Hallsworth, C., and J. Chisholm, 2008, Provenance of late Carboniferous sandstones in the Pennine Basin (UK) from combined heavy mineral, garnet geochemistry and palaeocurrent studies: Sedimentary Geology, v. 203, no. 3–4, p. 196–212, doi:10.1016/j.sedgeo.2007.11.002.
Hao, F., S. Li, Z. Gong, and J. Yang, 2000, Thermal regime, interreservoir compositional heterogeneities, and reservoir-filling history of the Dongfang gas field, Yinggehai basin, South China sea: Evidence for episodic fluid injections in overpressured basins?: AAPG Bulletin, v. 84, no. 5, p. 607–626, doi:10.1306/C9EBCE69-1735-11D7-8645000102C1865D.
Hao, F., Y. Sun, S. Li, and Q. Zhang, 1995, Overpressure retardation of organic-matter maturation and petroleum generation: A case study from the Yinggehai and Qiongdongnan Basins, South China Sea: AAPG Bulletin, v. 79, no. 4, p. 551–562, doi:10.1306/8D2B158E-171E-11D7-8645000102C1865D.
He, J., B. Xia, S. Zhang, and B. Liu, 2005, Hidden reservoir types and main hydocarbon accumulation factors in Yingdong Slop of Yinggehai Basin: Haiyang Dizhi Yu Disiji Dizhi, v. 25, p. 101–107, doi:10.16562/j.cnki.0256-1492.2005.02.016.
He, L., L. Xiong, and J. Wang, 2002, Heat flow and thermal modeling of the Yinggehai Basin, South China Sea: Tectonophysics, v. 351, no. 3, p. 245–253, doi:10.1016/S0040-1951(02)00160-9.
He, M., H. Zheng, and P. D. Clift, 2013, Zircon U-Pb geochronology and Hf isotope data from the Yangtze River sands: Implications for major magmatic events and crustal evolution in Central China: Chemical Geology, v. 360–361, p. 186–203, doi:10.1016/j.chemgeo.2013.10.020.
Hoang, L. V., P. D. Clift, D. Mark, H. Zheng, and M. T. Tan, 2010a, Ar-Ar muscovite dating as a constraint on sediment provenance and erosion processes in the Red and Yangtze River systems, SE Asia: Earth and Planetary Science Letters, v. 295, no. 3–4, p. 379–389, doi:10.1016/j.epsl.2010.04.012.

Hoang, L. V., P. D. Clift, A. M. Schwab, M. Huuse, D. A. Nguyen, and S. Zhen, 2010b, Large-scale erosional response of SE Asia to monsoon evolution reconstructed from sedimentary records of the Song Hong-Yinggehai and Qiongdongnan basins, South China Sea, *in* P. D. Clift, R. Tada, and H. Zheng, eds., Monsoon evolution and tectonics—Climate linkage in Asia: Geological Society, London, Special Publications 2010, v. 342, p. 219–244, doi:10.1144/SP342.13.

Hoang, L. V., F. Wu, P. D. Clift, A. Wysocka, and A. Swierczewska, 2009, Evaluating the evolution of the Red River system based on in situ U-Pb dating and Hf isotope analysis of zircons: Geochemistry Geophysics Geosystems, v. 10, doi:10.1029/2009GC002819.

Huang, B., X. Xiao, X. Li, and D. Cai, 2009, Spatial distribution and geochemistry of the nearshore gas seepages and their implications to natural gas migration in the Yinggehai Basin, offshore South China Sea: Marine and Petroleum Geology, v. 26, no. 6, p. 928–935, doi:10.1016/j.marpetgeo.2008.04.009.

Huang, B., X. Xiao, and W. Zhu, 2004, Geochemistry, origin, and accumulation of CO_2 in natural gases of the Yinggehai Basin, offshore South China Sea: AAPG Bulletin, v. 88, no. 9, p. 1277–1293, doi:10.1306/04120403045.

Jackson, S. E., N. J. Pearson, W. L. Griffin, and E. A. Belousova, 2004, The application of laser ablation-inductively coupled plasma-mass spectrometry to in situ U-Pb zircon geochronology: Chemical Geology, v. 211, no. 1–2, p. 47–69, doi:10.1016/j.chemgeo.2004.06.017.

Jiang, T., L. Cao, X. Xie, Z. Wang, X. Li, Y. Zhang, D. Zhang, and H. Sun, 2015, Insights from heavy minerals and zircon U-Pb ages into the middle Miocene-Pliocene provenance evolution of the Yinggehai Basin, northwestern South China Sea: Sedimentary Geology, v. 327, p. 32–42, doi:10.1016/j.sedgeo.2015.07.011.

Jonell, T. N., P. D. Clift, L. V. Hoang, T. Hoang, A. Carter, H. Wittmann, P. Boning, K. Pahnke, and T. Rittenour, 2017, Controls on erosion patterns and sediment transport in a monsoonal, tectonically quiescent drainage, Song Gianh, central Vietnam: Basin Research, v. 29, p. 659–683, doi:10.1111/bre.12199.

Kamvong, T., K. Zaw, S. Meffre, R. Maas, H. Stein, and C. K. Lai, 2014, Adakites in the Truong Son and Loei fold belts, Thailand and Laos: Genesis and implications for geodynamics and metallogeny: Gondwana Research, v. 26, no. 1, p. 165–184, doi:10.1016/j.gr.2013.06.011.

Kong, P., Y. Zheng, and M. W. Caffee, 2012, Provenance and time constraints on the formation of the first bend of the Yangtze River: Geochemistry Geophysics Geosystems, v. 13, no. 6, 15 p., doi:10.1029/2012GC004140.

Lei, C., J. Ren, P. D. Clift, Z. Wang, X. Li, and C. Tong, 2011, The structure and formation of diapirs in the Yinggehai-Song Hong Basin, South China Sea: Marine and Petroleum Geology, v. 28, no. 5, p. 980–991, doi:10.1016/j.marpetgeo.2011.01.001.

Lei, C., J. Ren, P. Sternai, M. Fox, S. Willett, X. Xie, P. D. Clift, J. Liao, and Z. Wang, 2015, Structure and sediment budget of Yinggehai-Song Hong basin, South China Sea: Implications for Cenozoic tectonics and river basin reorganization in Southeast Asia: Tectonophysics, v. 655, p. 177–190, doi:10.1016/j.tecto.2015.05.024.

Leloup, P. H., R. Lacassin, P. Tapponnier, U. Schärer, D. Zhong, X. Liu, L. Zhang, S. Ji, and P. T. Trinh, 1995, The Ailao Shan-Red River shear zone (Yunnan, China), tertiary transform boundary of Indochina: Tectonophysics, v. 251, no. 1–4, p. 3–84, doi:10.1016/0040-1951(95)00070-4.

Li, J., X. Fang, C. Song, B. Pan, Y. Ma, and M. Yan, 2014, Late Miocene-Quaternary rapid stepwise uplift of the NE Tibetan Plateau and its effects on climatic and environmental changes: Quaternary Research, v. 81, no. 3, p. 400–423, doi:10.1016/j.yqres.2014.01.002.

Li, X., S. Chung, H. Zhou, C. Lo, Y. Liu, and C. Chen, 2004, Jurassic intraplate magmatism in southern Hunan-eastern Guangxi: $^{40}Ar/^{39}Ar$ dating, geochemistry, Sr-Nd isotopes and implications for the tectonic evolution of SE China, *in* J. Malpas, C. J. N. Fletcher, J. R. Ali, and J. C. Aitchison, eds., Aspects of the tectonic evolution of China: Geological Society, London, Special Publications 2004, v. 226, p. 193–215, doi:10.1144/GSL.SP.2004.226.01.11.

Li, X. H., Z. X. Li, B. He, W. X. Li, Q. L. Li, Y. Gao, and X. C. Wang, 2012, The Early Permian active continental margin and crustal growth of the Cathaysia Block: In situ U-Pb, Lu-Hf and O isotope analyses of detrital zircons: Chemical Geology, v. 328, p. 195–207, doi:10.1016/j.chemgeo.2011.10.027.

Li, Z., X. Li, P. Kinny, J. Wang, S. Zhang, and H. Zhou, 2003, Geochronology of Neoproterozoic syn-rift magmatism in the Yangtze Craton, South China and correlations with other continents: Evidence for a mantle superplume that broke up Rodinia: Precambrian Research, v. 122, no. 1–4, p. 85–109, doi:10.1016/S0301-9268(02)00208-5.

Li, Z., X. Li, W. Li, and S. Ding, 2008, Was Cathaysia part of Proterozoic Laurentia? - New data from Hainan Island, south China: Terra Nova, v. 20, no. 2, p. 154–164, doi:10.1111/j.1365-3121.2008.00802.x.

Li, Z., X. Li, J. A. Wartho, C. Clark, W. Li, C. Zhang, and C. Bao, 2010, Magmatic and metamorphic events during the early Paleozoic Wuyi-Yunkai orogeny, southeastern South China: New age constraints and pressure-temperature conditions: Geological Society of America Bulletin, v. 122, no. 5–6, p. 772–793, doi:10.1130/B30021.1.

Liang, Y. H., S. L. Chung, D. Liu, Y. Xu, F. Y. Wu, J. H. Yang, Y. Wang, and C. H. Lo, 2008, Detrital zircon evidence from Burma for reorganization of the eastern Himalayan river system: American Journal of Science, v. 308, no. 4, p. 618–638, doi:10.2475/04.2008.08.

Liu, J., M. D. Tran, Y. Tang, Q. L. Nguyen, T. H. Tran, W. Wu, J. Chen, Z. Zhang, and Z. Zhao, 2012, Permo-Triassic granitoids in the northern part of the Truong Son belt, NW Vietnam: Geochronology, geochemistry and tectonic implications: Gondwana Research, v. 22, no. 2, p. 628–644, doi:10.1016/j.gr.2011.10.011.

Liu, R., J. Liu, W. Zhu, F. Hao, Y. Xie, Z. Wang, and L. Wang, 2016, In situ stress analysis in the Yinggehai Basin, northwestern South China Sea: Implication for the pore pressure-stress coupling process: Marine and Petroleum Geology, v. 77, p. 341–352, doi:10.1016/j.marpetgeo.2016.06.008.

Liu, S., R. Hu, S. Gao, C. Feng, Z. Huang, S. Lai, H. Yuan, et al., 2009, U-Pb zircon, geochemical and Sr-Nd-Hf isotopic constraints on the age and origin of Early Palaeozoic I-type granite from the Tengchong-Baoshan Block, Western Yunnan Province, SW China: Journal of Asian Earth Sciences, v. 36, no. 2–3, p. 168–182, doi:10.1016/j.jseaes.2009.05.004.

Liu, Y., S. Gao, Z. Hu, C. Gao, K. Zong, and D. Wang, 2010, Continental and oceanic crust recycling-induced melt-peridotite interactions in the trans-north China Orogen: U-Pb dating, Hf isotopes and trace elements in zircons from mantle xenoliths: Journal of Petrology, v. 51, no. 1–2, p. 537–571, doi:10.1093/petrology/egp082.

Lowe, D. G., P. J. Sylvester, and M. E. Enachescu, 2011, Provenance and paleodrainage patterns of Upper Jurassic and Lower Cretaceous synrift sandstones in the Flemish Pass Basin, offshore Newfoundland, east coast of Canada: AAPG Bulletin, v. 95, no. 8, p. 1295–1320, doi:10.1306/12081010005.

Miller, K. G., M. A. Kominz, J. V. Browning, J. D. Wright, G. S. Mountain, M. E. Katz, P. J. Sugarman, B. S. Cramer, N. Christie-Blick, and S. F. Pekar, 2005, The Phanerozoic record of global sea-level change: Science, v. 310, p. 1293–1298, doi:10.1126/science.1116412.

Milliman, J. D., C. M. Rutkowski, and M. Meybeck, 1995, River discharge to the sea: A global river index: Texel, the Netherlands, Land–Ocean Interactions in the Coastal Zone Core Project Office, 125 p.

Morley, C. K., 2002, A tectonic model for the Tertiary evolution of strike-slip faults and rift basins in SE Asia: Tectonophysics, v. 347, no. 4, p. 189–215, doi:10.1016/S0040-1951(02)00061-6.

Morton, A., M. Fanning, and P. Milner, 2008, Provenance characteristics of Scandinavian basement terrains: Constraints from detrital zircon ages in modern river sediments: Sedimentary Geology, v. 210, no. 1–2, p. 61–85, doi:10.1016/j.sedgeo.2008.07.001.

Pruszak, Z., M. Szmytkiewicz, N. M. Hung, and P. V. Ninh, 2002, Coastal processes in the Red River delta area, Vietnam: Coastal Engineering Journal, v. 44, no. 2, p. 97–126, doi:10.1142/S0578563402000469.

Rangin, C., M. Klein, D. Roques, X. Le Pichon, and L. V. Trong, 1995, The Red River fault system in the Tonkin Gulf, Vietnam: Tectonophysics, v. 243, no. 3–4, p. 209–222, doi:10.1016/0040-1951(94)00207-P.

Replumaz, A., R. Lacassin, P. Tapponnier, and P. H. Leloup, 2001, Large river offsets and Plio-Quaternary dextral slip rate on the Red River fault (Yunnan, China): Journal of Geophysical Research: Solid Earth, v. 106, no. B1, p. 819–836, doi:10.1029/2000JB900135.

Roger, F., N. Arnaud, S. Gilder, P. Tapponnier, M. Jolivet, M. Brunel, J. Malavieille, Z. Xu, and J. Yang, 2003, Geochronological and geochemical constraints on Mesozoic suturing in east central Tibet: Tectonics, v. 22, no. 4, 20 p., doi:10.1029/2002TC001466.

Roger, F., H. Maluski, A. Leyreloup, C. Lepvrier, and P. T. Thi, 2007, U-Pb dating of high temperature metamorphic episodes in the Kon Tum Massif (Vietnam): Journal of Asian Earth Sciences, v. 30, no. 3–4, p. 565–572, doi:10.1016/j.jseaes.2007.01.005.

Rudnick, R. L., and I. S. Williams, 1987, Dating the lower crust by ion microprobe: Earth and Planetary Science Letters, v. 85, no. 1–3, p. 145–161, doi:10.1016/0012-821X(87)90028-8.

Schoenbohm, L. M., B. C. Burchfiel, and L. Chen, 2006, Propagation of surface uplift, lower crustal flow, and Cenozoic tectonics of the southeast margin of the Tibetan Plateau: Geology, v. 34, no. 10, p. 813–816, doi:10.1130/G22679.1.

Searle, M. P., 2006, Role of the Red River Shear zone, Yunnan and Vietnam, in the continental extrusion of SE Asia: Journal of the Geological Society, v. 163, no. 6, p. 1025–1036, doi:10.1144/0016-76492005-144.

Sircombe, K. N., W. Bleeker, and R. A. Stern, 2001, Detrital zircon geochronology and grain-size analysis of a ~2800 Ma Mesoarchean proto-cratonic cover succession, Slave Province, Canada: Earth and Planetary Science Letters, v. 189, no. 3–4, p. 207–220, doi:10.1016/S0012-821X(01)00363-6.

Sun, M., H. Wang, J. Liao, H. Gan, J. Xiao, and J. Ren, 2014, Sedimentary characteristics and model of gravity flow depositional system for the first member of upper Miocene Huangliu Formation in Dongfang area, Yinggehai basin, northwestern South China Sea: Journal of Earth Science, v. 25, no. 3, p. 506–518, doi:10.1007/s12583-014-0451-5.

Sun, X., and P. Wang, 2005, How old is the Asian monsoon system?—Palaeobotanical records from China: Palaeogeography, Palaeoclimatology, Palaeoecology, v. 222, no. 3–4, p. 181–222, doi:10.1016/j.palaeo.2005.03.005.

Sun, Z., D. Zhou, Z. Zhong, Z. Zeng, and S. Wu, 2003, Experimental evidence for the dynamics of the formation of the Yinggehai basin, NW South China Sea: Tectonophysics, v. 372, no. 1–2, p. 41–58, doi:10.1016/S0040-1951(03)00230-0.

Tapponnier, P., Z. Xu, F. Roger, B. Meyer, N. Arnaud, G. Wittlinger, and J. Yang, 2001, Oblique stepwise rise and growth of the Tibet Plateau: Science, v. 294, no. 5547, p. 1671–1677, doi:10.1126/science.105978.

Usuki, T., C. Y. Lan, K. L. Wang, and H. Y. Chiu, 2013, Linking the Indochina block and Gondwana during the Early Paleozoic: Evidence from U-Pb ages and Hf isotopes of detrital zircons: Tectonophysics, v. 586, p. 145–159, doi:10.1016/j.tecto.2012.11.010.

Vermeesch, P., 2012, On the visualisation of detrital age distributions: Chemical Geology, v. 312–313, p. 190–194, doi:10.1016/j.chemgeo.2012.04.021.

Vermeesch, P., 2013, Multi-sample comparison of detrital age distributions: Chemical Geology, v. 341, p. 140–146, doi:10.1016/j.chemgeo.2013.01.010.

Vermeesch, P., 2014a, Corrigendum to “Multi-sample comparison of detrital age distributions” [Chem. Geol. 191 (2002) 209–224]: Chemical Geology, v. 363, p. 356.

Vermeesch, P., 2014b, Corrigendum to "Multi-sample comparison of detrital age distributions" [Chem. Geol. 341 (2013) 140–146]: Chemical Geology, v. 380, p. 191.
Vermeesch, P., 2016, Corrigendum to "Multi-sample comparison of detrital age distributions" [Chem. Geol. 341 (2013) 140–146]: Chemical Geology, v. 425, p. 145.
Wan, S., A. Li, P. D. Clift, and H. Jiang, 2006, Development of the East Asian summer monsoon: Evidence from the sediment record in the South China Sea since 8.5 Ma: Palaeogeography, Palaeoclimatology, Palaeoecology, v. 241, no. 1, p. 139–159, doi:10.1016/j.palaeo.2006.06.013.
Wang, C., X. Liang, D. A. Foster, J. Fu, Y. Jiang, C. Dong, Y. Zhou, S. Wen, and P. V. Quynh, 2016b, Detrital zircon U-Pb geochronology, Lu-Hf isotopes and REE geochemistry constrains on the provenance and tectonic setting of Indochina Block in the Paleozoic: Tectonophysics, v. 677–678, p. 125–134, doi:10.1016/j.tecto.2016.04.008.
Wang, C., X. Liang, D. A. Foster, Y. Xie, C. Tong, J. Pei, J. Fu, Y. Jiang, C. Dong, and Y. Zhou, 2016a, Zircon U-Pb geochronology and heavy mineral composition constraints on the provenance of the middle Miocene deepwater reservoir sedimentary rocks in the Yinggehai-Song Hong Basin, South China Sea: Marine and Petroleum Geology, v. 77, p. 819–834, doi:10.1016/j.marpetgeo.2016.05.009.
Wang, C., X. Liang, J. Fu, Y. Jiang, and C. Dong, 2016c, Detrital zircon U-Pb geochronology: New insight into the provenance of Sanya Formation in the Yinggehai Basin: Acta Geologica Sinica, v. 90, no. 1, p. 386–387, doi:10.1111/1755-6724.12667.
Wang, C., X. Liang, Y. Xie, C. Tong, J. Pei, Y. Zhou, Y. Jiang, J. Fu, C. Dong, and P. Liu, 2014, Provenance of Upper Miocene to Quaternary sediments in the Yinggehai-Song Hong Basin, South China Sea: Evidence from detrital zircon U-Pb ages: Marine Geology, v. 355, p. 202–217, doi:10.1016/j.margeo.2014.06.004.
Wang, C., X. Liang, Y. Xie, C. Tong, J. Pei, Y. Zhou, Y. Jiang, J. Fu, and S. Wen, 2015a, Late Miocene provenance change on the eastern margin of the Yinggehai-Song Hong Basin, South China Sea: Evidence from U-Pb dating and Hf isotope analyses of detrital zircons: Marine and Petroleum Geology, v. 61, p. 123–139, doi:10.1016/j.marpetgeo.2014.12.004.
Wang, C., X. Liang, Y. Zhou, J. Fu, Y. Jiang, C. Dong, Y. Xie, C. Tong, J. Pei, and P. Liu, 2015b, Construction of age frequencies of provenances on the eastern side of the Yinggehai Basin: Studies of LA-ICP-MS U-Pb ages of detrital zircons from six modern rivers, western Hainan, China: Earth Science Frontiers, v. 22, p. 277–289, doi:10.13745/j.esf.2015.04.028.
Wang, L., W. L. Griffin, J. Yu, and S. Y. O'Reilly, 2010, Precambrian crustal evolution of the Yangtze Block tracked by detrital zircons from Neoproterozoic sedimentary rocks: Precambrian Research, v. 177, no. 1–2, p. 131–144, doi:10.1016/j.precamres.2009.11.008.
Wang, X. L., J. C. Zhou, W. L. Griffin, R. C. Wang, J. S. Qiu, S. Y. O'Reilly, X. Xu, L. M. Liu, and G. L. Zhang, 2007a, Detrital zircon geochronology of Precambrian basement sequences in the Jiangnan orogen: Dating the assembly of the Yangtze and Cathaysia Blocks: Precambrian Research, v. 159, no. 1–2, p. 117–131, doi:10.1016/j.precamres.2007.06.005.
Wang, Y., W. Fan, G. Zhao, S. Ji, and T. Peng, 2007b, Zircon U-Pb geochronology of gneissic rocks in the Yunkai massif and its implications on the Caledonian event in the South China Block: Gondwana Research, v. 12, no. 4, p. 404–416, doi:10.1016/j.gr.2006.10.003.
Wang, Y., A. Zhang, W. Fan, G. Zhao, G. Zhang, Y. Zhang, F. Zhang, and S. Li, 2011, Kwangsian crustal anatexis within the eastern South China Block: Geochemical, zircon U-Pb geochronological and Hf isotopic fingerprints from the gneissoid granites of Wugong and Wuyi-Yunkai Domains: Lithos, v. 127, no. 1–2, p. 239–260, doi:10.1016/j.lithos.2011.07.027.
Wei, H. H., E. Wang, G. L. Wu, and K. Meng, 2016, No sedimentary records indicating southerly flow of the paleo-Upper Yangtze River from the First Bend in southeastern Tibet: Gondwana Research, v. 32, p. 93–104, doi:10.1016/j.gr.2015.02.006.
Weislogel, A. L., S. A. Graham, E. Z. Chang, J. L. Wooden, G. E. Gehrels, and H. Yang, 2006, Detrital zircon provenance of the Late Triassic Songpan-Ganzi complex: Sedimentary record of collision of the North and South China blocks: Geology, v. 34, no. 2, p. 97–100, doi:10.1130/G21929.1.
Wen, S., 2013, Geochronologic and geochemical studies of Permian-Triassic magmatism in Hainan Island, South China, Ph.D. thesis, University of Chinese Academy of Sciences, Beijing, China, 142 p.
Wissink, G. K., G. D. Hoke, C. N. Garzione, and Z. J. Liu, 2016, Temporal and spatial patterns of sediment routing across the southeast margin of the Tibetan Plateau: Insights from detrital zircon: Tectonics, v. 35, no. 11, p. 2538–2563, doi:10.1002/2016TC004252.
Xie, C., J. Zhu, S. Ding, Y. Zhang, and Z. Li, 2006, Identification of Hercynian shoshonitic intrusive rocks in central Hainan Island and its geotectonic implications: Chinese Science Bulletin, v. 51, no. 20, p. 2507–2519, doi:10.1007/s11434-006-2122-0.
Xie, Y., 2009, Sequence stratigraphic analysis and hydrocarbon accumulation models in tectonically active basins—Case study on the Yinggehai Basin: Beijing, China, Geological Publishing House, 147 p.
Xu, D., B. Xia, P. Li, G. Chen, C. Ma, and Y. Zhang, 2007a, Protolith natures and U-Pb sensitive high mass-resolution ion microprobe (SHRIMP) zircon ages of the metabasites in Hainan Island, South China: Implications for geodynamic evolution since the late Precambrian: Island Arc, v. 16, no. 4, p. 575–597, doi:10.1111/j.1440-1738.2007.00584.x.
Xu, X., S. Y. O'Reilly, W. L. Griffin, X. Wang, N. J. Pearson, and Z. He, 2007b, The crust of Cathaysia: Age, assembly and reworking of two terranes: Precambrian Research,

v. 158, no. 1–2, p. 51–78, doi:10.1016/j.precamres.2007.04.010.
Xu, Y., C. Y. Wang, and T. Zhao, 2016, Using detrital zircons from river sands to constrain major tectono-thermal events of the Cathaysia Block, SE China: Journal of Asian Earth Sciences, v. 124, p. 1–13, doi:10.1016/j.jseaes.2016.04.012.
Yan, Y., A. Carter, C. Palk, S. Brichau, and X. Hu, 2011, Understanding sedimentation in the Song Hong-Yinggehai Basin, South China Sea: Geochemistry Geophysics Geosystems, v. 12, no. 6, 15 p., doi:10.1029/2011GC003533.
Yan, Y., B. Xia, G. Lin, A. Carter, X. Hu, X. Cui, B. Liu, P. Yan, and Z. Song, 2007, Geochemical and Nd isotope composition of detrital sediments on the north margin of the South China Sea: Provenance and tectonic implications: Sedimentology, v. 54, no. 1, p. 1–17, doi:10.1111/j.1365-3091.2006.00816.x.
Yang, S., F. Zhang, and Z. Wang, 2012, Grain size distribution and age population of detrital zircons from the Changjiang (Yangtze) River system, China: Chemical Geology, v. 296–297, p. 26–38, doi:10.1016/j.chemgeo.2011.12.016.
Yao, J., L. Shu, and M. Santosh, 2011, Detrital zircon U-Pb geochronology, Hf-isotopes and geochemistry—New clues for the Precambrian crustal evolution of Cathaysia Block, South China: Gondwana Research, v. 20, no. 2–3, p. 553–567, doi:10.1016/j.gr.2011.01.005.
Yu, J. H., S. Y. O'Reilly, L. Wang, W. L. Griffin, M. Zhang, R. Wang, S. Jiang, and L. Shu, 2008, Where was South China in the Rodinia supercontinent?: Evidence from U-Pb geochronology and Hf isotopes of detrital zircons: Precambrian Research, v. 164, no. 1–2, p. 1–15, doi:10.1016/j.precamres.2008.03.002.
Yu, J. H., L. Wang, S. Y. O'Reilly, W. L. Griffin, M. Zhang, C. Li, and L. Shu, 2009, A Paleoproterozoic orogeny recorded in a long-lived cratonic remnant (Wuyishan terrane), eastern Cathaysia Block, China: Precambrian Research, v. 174, no. 3–4, p. 347–363, doi:10.1016/j.precamres.2009.08.009.
Zhai, Q. G., B. M. Jahn, R. Y. Zhang, J. Wang, and L. Su, 2011, Triassic subduction of the Paleo-Tethys in northern Tibet, China: Evidence from the geochemical and isotopic characteristics of eclogites and blueschists of the Qiangtang Block: Journal of Asian Earth Sciences, v. 42, no. 6, p. 1356–1370, doi:10.1016/j.jseaes.2011.07.023.
Zhang, L., and U. Schärer, 1999, Age and origin of magmatism along the Cenozoic Red River shear belt, China: Contributions to Mineralogy and Petrology, v. 134, no. 1, p. 67–85, doi:10.1007/s004100050469.
Zhang, P. Z., P. Molnar, and W. R. Downs, 2001, Increased sedimentation rates and grain sizes 2-4 Myr ago due to the influence of climate change on erosion rates: Nature, v. 410, no. 6831, p. 891–897, doi:10.1038/35073504.
Zhang, Q. M., F. N. Liu, and J. H. Yang, 1996, The relationship of overpressured system with oil and gas migration in the Yinggehai Basin: China Offshore: Oil, Gas (Hamburg), v. 10, p. 65–75.
Zhao, M., L. Shao, J. Liang, and Q. Li, 2015a, No Red River capture since the late Oligocene: Geochemical evidence from the Northwestern South China Sea: Deep-sea Research. Part II, Topical Studies in Oceanography, v. 122, p. 185–194, doi:10.1016/j.dsr2.2015.02.029.
Zhao, M., L. Shao, and P. Qiao, 2015b, Characteristics of detrital zircon U-Pb geochronology of the Pearl River Sands and its implication on provenances: Journal of Tongji University, v. 43, p. 89–97, doi:10.11908/j.issn.0253-374x.2015.06.018.
Zheng, H., P. D. Clift, P. Wang, R. Tada, J. Jia, M. He, and F. Jourdan, 2013, Pre-Miocene birth of the Yangtze River: Proceedings of the National Academy of Sciences of the United States of America, v. 110, no. 19, p. 7556–7561, doi:10.1073/pnas.1216241110.
Zheng, J., W. Griffin, S. Y. O'Reilly, M. Zhang, N. Pearson, and Y. Pan, 2006, Widespread Archean basement beneath the Yangtze craton: Geology, v. 34, no. 6, p. 417–420, doi:10.1130/G22282.1.
Zhou, J., X. H. Li, W. Ge, and Z. X. Li, 2007, Age and origin of middle Neoproterozoic mafic magmatism in southern Yangtze Block and relevance to the break-up of Rodinia: Gondwana Research, v. 12, no. 1–2, p. 184–197, doi:10.1016/j.gr.2006.10.011.
Zhou, Y., X. Liang, A. Kröner, Y. Cai, T. Shao, S. Wen, Y. Jiang, J. Fu, C. Wang, and C. Dong, 2015, Late Cretaceous lithospheric extension in SE China: Constraints from volcanic rocks in Hainan Island: Lithos, v. 232, p. 100–110, doi:10.1016/j.lithos.2015.06.028.
Zhu, M., S. Graham, and T. McHargue, 2009, The red river fault zone in the Yinggehai Basin, South China Sea: Tectonophysics, v. 476, no. 3–4, p. 397–417, doi:10.1016/j.tecto.2009.06.015.
Zhu, W., and C. Lei, 2013, Refining the model of South China Sea's tectonic evolution: Evidence from Yinggehai-Song Hong and Qiongdongnan Basins: Marine Geophysical Researches, v. 34, no. 3–4, p. 325–339, doi:10.1007/s11001-013-9202-8.